Environmental Science Advances

ROYAL SOCIETY OF CHEMISTRY

PAPER

View Article Online
View Journal | View Issue

Open Access Article. Published on 15 August 2025. Downloaded on 2/27/2026 8:14:49 PM.
This article is licensed under a Creative Commons Attribution-NonCommercial 3.0 Unported Licence.

Check for updates

Cite this: *Environ. Sci.: Adv.*, 2025, **4**, 1663

Does the carbon pool vary among Ecuador's tropical dry forests and seasons? Experimental evidence from spatio-temporal assessments

Michael Macías-Pro, *[ab] Emilio Jarre Castro, [a] Juan Manuel Moreira Castro,[c] José María Montoya Terán [b] and Ezequiel Zamora-Ledezma *[a]

Received 24th January 2025
Accepted 12th August 2025

DOI: 10.1039/d5va00018a

rsc.li/esadvances

Tropical dry forests (TDFs) are critical carbon reservoirs, yet their carbon storage dynamics remain poorly understood, particularly across seasons, forest subtypes, and species' contributions. This study examined carbon pools—soil organic carbon (SOC), aboveground biomass carbon (CAGB), and litterfall carbon (C-litterfall)—across three TDF subtypes along the Ecuadorian coast. Twelve 100 m^2 plots were monitored semi-annually during rainy and dry seasons, with extrapolations made to assess total forest patch carbon stocks. SOC was the dominant carbon pool across all subtypes and seasons, with rainy periods contributing to greater SOC stability (LSF, 75.51 Mg ha^{-1}; LDF, 70.01 Mg ha^{-1}; SPF, 69.27 Mg ha^{-1}) compared to dry periods (LDF, 54.70 Mg ha^{-1}; LSF, 53.35 Mg ha^{-1}; SPF, 39.39 Mg ha^{-1}). CAGB and C-litterfall displayed significant seasonal variation, with litterfall peaking in the dry season, particularly in LSF (0.4 Mg ha^{-1}). Across subtypes, total carbon densities averaged 94.0 Mg ha^{-1} in LSF, 67.4 Mg ha^{-1} in SPF, and 99.9 Mg ha^{-1} in LDF. Plant species significantly influenced CAGB. In LSF, *T. integerrima* contributed the most to CAGB (6.4–6.7 Mg ha^{-1}), while *C. eggersii* dominated in SPF (4.5–4.4 Mg ha^{-1}). In LDF, *C. lutea* was the leading contributor, storing 13.8–13.9 Mg ha^{-1} of biomass carbon. Extrapolation to forest patches revealed substantial spatial differences, with LDF sequestering the most carbon (526 133.3 Mg), followed by SPF (463 133.0 Mg) and LSF (3113.3 Mg). These findings underscore the critical roles of species composition, climatic variability, and forest structure in carbon sequestration, emphasizing the need for tailored conservation strategies to mitigate climate change impacts.

Environmental significance

Tropical dry forests are critical for carbon cycling and climate regulation, yet they remain understudied compared to humid tropical forests. This research investigates spatio-temporal variations in carbon pools—soil organic carbon, aboveground biomass, and litterfall—across three Ecuadorian TDF subtypes. Findings reveal the influence of seasonality, forest structure, and species composition on carbon storage, emphasizing SOC as the dominant pool and litterfall's role in nutrient cycling. By addressing these dynamics under climate and anthropogenic pressures, this study provides actionable insights for conservation strategies and sustainable land management. The results contribute to bridging knowledge gaps in TDF carbon dynamics, supporting efforts to mitigate climate change and to preserve these endangered ecosystems.

1 Introduction

Forests are essential components of the global carbon cycle and play a pivotal role in mitigating climate change by serving as natural carbon sinks.[1] Globally, forests store approximately 662 billion tons of carbon, accounting for nearly 80% of terrestrial carbon stocks in biomass and soil organic matter.[2] Through photosynthesis, forests absorb atmospheric CO_2, release oxygen, and sequester carbon into plant biomass and soils, thereby contributing to long-term carbon storage and supporting ecosystem services.[3,4] Tropical forests cover merely 7% of the Earth's land surface and harbour more than half of the world's biodiversity.[5,6] These forests are highly threatened by human activities including forest fires.[5,7,8] They are particularly significant, as they store nearly 50% of terrestrial carbon and regulate global climate processes.[9,10] However, deforestation, degradation, and the intensifying impacts of climate change threaten their ability to function as net carbon sinks, with some tropical forests transitioning into net carbon sources.[11–13]

Among tropical forest subtypes, TDFs play an equally critical, yet often overlooked, role in global carbon dynamics. TDFs

[a]*Laboratorio Funcionamiento de Agroecosistemas y Cambio Climático – FAGROCLIM, Departamento de Ciencias Agrícolas, Facultad de Ingeniería Agrícola, Universidad Técnica de Manabí (UTM), Lodana, 13132, Ecuador. E-mail: michael.macias@utm.edu.ec; ezequiel.zamora@utm.edu.ec*

[b]*Theoretical and Experimental Ecological Station, CNRS, UPS, Moulis, France*

[c]*Jardín Universitario, Universidad Técnica de Manabí (UTM), Portoviejo, 130105, Ecuador*

Open Access Article. Published on 15 August 2025. Downloaded on 2/27/2026 8:14:49 PM.
This article is licensed under a Creative Commons Attribution-NonCommercial 3.0 Unported Licence.

account for approximately 40% of all tropical forests and harbor substantial biodiversity, unique ecosystem services, and carbon pools.[14–16] In addition to supporting diverse livelihoods, TDFs regulate climate through the sequestration and cycling of atmospheric carbon in their biomass, soil organic carbon (SOC), and leaf litter.[17,18] These forests are particularly vulnerable to environmental and anthropogenic stressors, including deforestation, unsustainable land-use practices, and climate variability. This has led to TDFs being classified among the most endangered ecosystems globally, with high rates of fragmentation and limited representation in protected areas.[19,20]

SOC is a fundamental component of soil health and ecosystem functioning, influencing nutrient cycling, water retention, and overall fertility.[21–23] Globally, soils store approximately 1500–2000 Pg of organic carbon, nearly double the amount of carbon held in the atmosphere and vegetation combined.[24,25] SOC also plays a critical role in mitigating climate change by serving as a long-term carbon reservoir.[26] However, SOC stocks are highly dynamic and sensitive to changes in temperature, precipitation, vegetation cover, and human activities.[27,28] The impacts of climate change, including rising temperatures, altered precipitation patterns, and extreme weather events (*e.g.*, El Niño-Southern Oscillation), have led to significant SOC losses globally, estimated at 0.3–1 Pg per year.[29,30]

In TDFs, SOC dynamics are further influenced by spatial (*e.g.*, forest subtypes and soil depth) and temporal (*e.g.*, seasonal changes) variations. Precipitation seasonality plays a critical role in determining SOC inputs and outputs, such as litterfall production, microbial decomposition, and carbon mineralization rates.[31,32] In the dry season, limited water availability can constrain biological activity, slowing down organic matter decomposition and nutrient cycling, while the wet period may enhance SOC turnover but also increase leaching and soil erosion risks.[33,34]

Similarly, SOC pools vary significantly with soil depth, with surface layers generally containing higher carbon concentrations due to organic matter inputs from litterfall and root biomass, whereas deeper layers may store older, more stable carbon fractions.[35,36] Despite this variability, detailed assessments of SOC dynamics across soil profiles and seasonal periods remain limited in TDFs.

In addition to SOC, aboveground biomass (AGB) and litterfall production are critical components of TDF carbon cycling. AGB acts as a temporary carbon sink, storing atmospheric carbon in plant tissues, while litterfall serves as the primary pathway for organic carbon input into the soil.[37–40] Litter decomposition not only replenishes soil nutrients but also influences microbial activity, soil fertility, and ecosystem recovery following disturbances.[41,42] Understanding the interplay between these carbon pools—AGB, SOC, and litterfall—is crucial for assessing the carbon balance of TDFs, particularly under the dual pressures of climate change and anthropogenic disturbance.

Despite their ecological and climate-regulating importance, TDFs have received considerably less scientific attention compared to humid tropical forests. This knowledge gap hinders the development of effective conservation and management strategies for these ecosystems, which face some of the highest deforestation and degradation rates globally.[11,43] Bridging this gap requires detailed, region-specific studies that investigate the spatio-temporal variations in carbon pools across TDF landscapes.

In this study, we address this critical research need by examining the spatio-temporal variations in carbon pools (SOC, AGB, and C-litterfall) in Ecuador's TDFs, with a specific focus on differences across three TDF subtypes and seasonal periods. By integrating analyses of carbon dynamics trends, this research provides insights into the role of TDFs in carbon cycling and their potential contributions to climate change mitigation. The findings aim to support evidence-based conservation strategies and sustainable land management practices for these threatened ecosystems; thus, we hypothesize that carbon pools in Ecuadorian tropical dry forests differ significantly across forest subtypes and seasonal periods, driven by climatic seasonality, forest structure, and species composition.

2 Materials and methods

2.1 Study sites and plot distribution

This research was conducted in three subtypes of tropical dry forests (TDFs) along the Pacific Ecuadorian coast. The study sites were chosen to encompass differences in environmental conditions, plant diversity and physical–chemical soil characteristics along a geographical gradient (north to south). Three TDF subtypes were studied: (i) Jama-Zapotillo Lowland Semi-deciduous Forest (LSF) located in Sua (Esmeraldas province); (ii) Deciduous Pacific Forest of the Equatorial Coast (SPF) found in Pacoche (Manabí province); and (iii) Lowland Deciduous Forest and Shrubland of Jama-Zapotillo (LDF) in Manglaralto (Santa Elena province) (Fig. 1). All subtypes face threats such as deforestation, fire, vegetation replacement by crops and livestock, soil erosion, and urban expansion.[44]

In the tree forests (LSF, SPF and LDF), a total of twelve permanent experimental plots ($n = 12$) of 100 m^2 (10×10 m), were established (4 plots per site; P1 to P12), with a minimum separation of 60 meters between plots within the same site. In all plots, different measures were taken to characterize the plant community and soil attributes from January to December 2022, specifically, during two field campaigns corresponding to the rainy period (January to May) and the dry period (June to December).[45]

The three forest subtypes analyzed in this study exhibit distinct climatic conditions, physiognomies, and ecological features, shaped by their varied biogeographical settings and the pronounced climatic gradient along the Ecuadorian coast, as shown in Table 1.[46] From the wetter, subhumid north to the drier, xeric south, differences in rainfall and temperature significantly influence vegetation structure and species composition. The study design incorporated spatial and temporal variations to assess how these ecosystems respond to seasonal dynamics and variations along the latitudinal gradient.

 © 2025 The Author(s). Published by the Royal Society of Chemistry

Open Access Article. Published on 15 August 2025. Downloaded on 2/27/2026 8:14:49 PM.
This article is licensed under a Creative Commons Attribution-NonCommercial 3.0 Unported Licence.

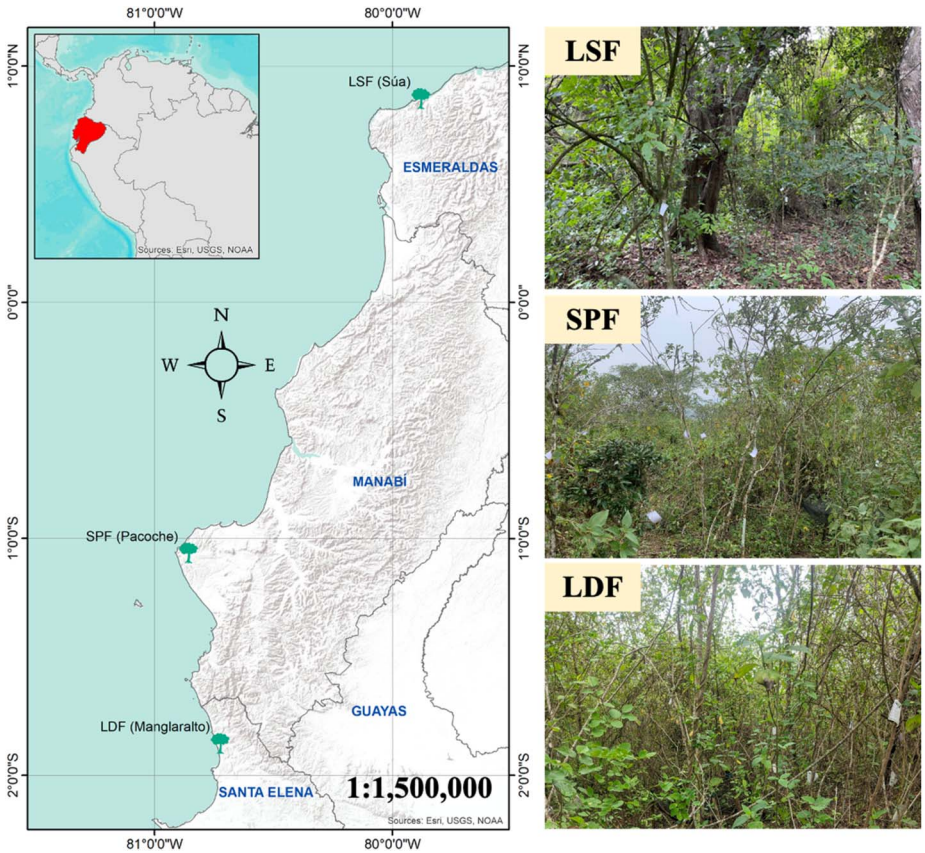

Fig. 1 Relative location of the forest subtypes along the Ecuadorian coast. LSF: Jama-Zapotillo Lowland Semideciduous Forest (Esmeraldas province); SPF: Deciduous Pacific Forest of the Equatorial Coast (Manabí province); LDF: Lowland Deciduous Forest and Shrubland of Jama-Zapotillo (Santa Elena province).

2.2 Ecological and climatic characterization of tropical dry forest subtypes

The tropical dry forest (TDF) subtypes exhibit distinct ecological and climatic characteristics that shape their biodiversity and landscape dynamics (Table 1, SI 1).

The Jama-Zapotillo Lowland Semideciduous Forest (LSF), spanning 287 hectares, is characterized by a semi-deciduous physiognomy within a pluvial seasonal subhumid bioclimate. It presents relatively humid conditions compared to other subtypes.

In contrast, the Deciduous Pacific Forest of the Equatorial Coast (SPF) is much larger, covering 41 122.7 hectares within the Pacific Equatorial Province. This deciduous forest is marked by a xeric bioclimate and a dry ombrotype, reflecting significantly drier conditions.

The Lowland Deciduous Forest and Shrubland of Jama-Zapotillo (LDF) is the largest forest subtype, encompassing 227 757.7 hectares. This ecosystem consists of forest and shrubland with a low forest physiognomy in a xeric bioclimate and dry ombrotype. The LDF spans diverse terrain, including foothills, coastal plains, beaches, and hillslopes.

Together, these subtypes represent the ecological heterogeneity of TDFs, influenced by climatic and geomorphological gradients.

2.3 Soil sampling design and analyses

To provide an edaphic context for the studied forest subtypes, some soil parameters were analyzed to characterize the physical and chemical properties of the sites. Key soil attributes, including electrical conductivity (EC), pH, and soil bulk density (SBD), were evaluated at two depth intervals (0–40 cm and 40–80 cm) to capture depth-wise variations in soil characteristics. Within each plot, a zigzag transect design was used to ensure representative sampling. Three transects were established, each with six sampling points spaced 100 cm apart, resulting in nine sampling points per plot (Fig. 2). At each sampling point, soil cores were collected from both depth intervals using a metallic soil core sampler (15 cm diameter; 40 cm length). The collected samples were immediately placed in labeled plastic bags, kept in a cooler with frozen gel packs, and transported to the laboratory for analysis.

2.4 Physico-chemical analyses of soil

In the laboratory, soil samples were dried according to ISO 11461:2001 standards.[47] Drying was performed using a Memmert UN30 oven at 50 °C for approximately 24 hours. Subsequently, samples were stabilized in a dry chamber with desiccant material at 23 °C for 30 minutes to ensure constant

Open Access Article. Published on 15 August 2025. Downloaded on 2/27/2026 8:14:49 PM.
This article is licensed under a Creative Commons Attribution-NonCommercial 3.0 Unported Licence.

Table 1 Forest subtypes: biophysics attributes and description. MAT: mean annual temperature; MAP: mean annual precipitation

Forest subtype	Patch area (ha)	MAT (°C)	MAP (mm)	Altitude (m.a.s.l.)	Features
Jama-Zapotillo Lowland Semideciduous Forest (LSF)	33.1	25.2	1445	0–300	The area features a semi-deciduous physiognomy in a pluvial seasonal subhumid bioclimate. Situated in lowlands with an infratropical thermotype, it lies in a non-floodable alluvial plain within the Jama-Zapotillo sector. Additionally, the forest has remained unaffected by human activities for the past 22 years
Deciduous Pacific Forest of the Equatorial Coast (SPF)	6871.4	23.2	829	200–300	The area is a deciduous forest located in the Coastal Region of the Pacific Equatorial Province, with a xeric bioclimate and dry ombrotype. It features a coastal relief with mountains and piedmont. Additionally, the area has remained untouched for the past 9 years
Lowland Deciduous Forest and Shrubland of Jama-Zapotillo (LDF)	5266.6	25.5	702	0–400	The area comprises forest and shrubland, featuring a low forest physiognomy, situated in the Coastal Region, Pacific Equatorial Province, Jama-Zapotillo sector. It possesses a xeric bioclimate, dry ombrotype, and is deciduous, located within lowlands with an infratropical thermotype. The relief is coastal, including foothills, plains, coastal plains, beaches, and hillslopes, and it has remained untouched for approximately 17 years

weight. The dried soil samples were ground and passed through a 2 mm mesh sieve.

Electrical conductivity and pH were measured following the standards UNE 77308:2001[48] and UNE-EN ISO 10390:2022.[49] 10 grams of soil were weighed in an Erlenmeyer flask, 50 mL of deionized water were added, and the mixture was shaken in a BT921 shaker at 200 rpm for 30 minutes. Subsequently, filtration was performed using a "Sartorius" filter paper with a pore size of 0.45 μm and a vacuum filtration setup (Kitasato Flask) connected to a "GAST" diaphragm vacuum-pressure pump with a maximum pressure of 4.1 bar. Finally, the obtained extracts were used to measure both pH and EC (μS cm^{-1}) using a multiparameter WTW, model pH/Cond 3320 SET.

Soil bulk density was determined according to UNE-EN ISO 11272:2017.[47] A 50 mL Falcon polypropylene tube was filled with 10 g of soil and weighed using an OHAUS (eqn (1)).

$$\mathrm{SBD} = \frac{D_{\mathrm{sw}}}{\mathrm{Vol_c}} \tag{1}$$

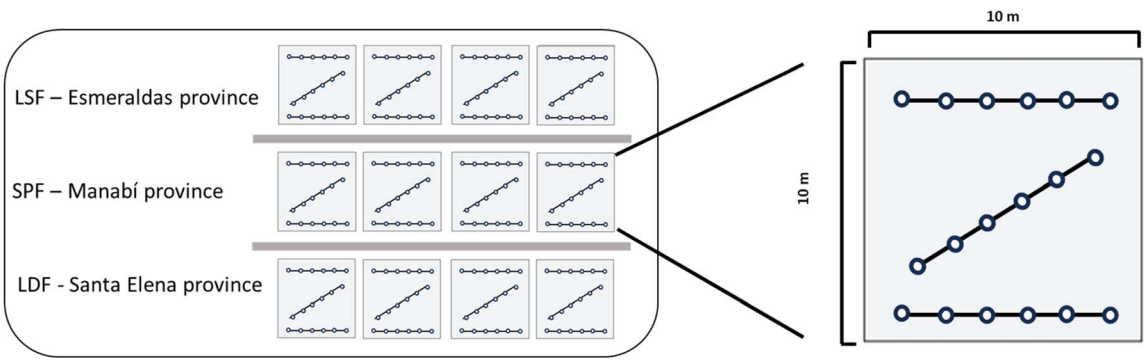

Fig. 2 Spatial design of the transects in plots of the TDF subtypes. LSF (Jama-Zapotillo Lowland Semideciduous Forest), SPF (Deciduous Pacific Forest of the Equatorial Coast), and LDF (Lowland Deciduous Forest and Shrubland of Jama-Zapotillo)—were represented by four permanent plots (10 × 10 m), for a total of twelve plots. Within each plot, three parallel transects were established. Along each transect, six regularly spaced sampling points were fixed, resulting in 18 sampling points per plot. Soil samples were collected at each point and at two depths (0–40 cm and 40–80 cm) to assess vertical variation in soil organic carbon.

 © 2025 The Author(s). Published by the Royal Society of Chemistry

Open Access Article. Published on 15 August 2025. Downloaded on 2/27/2026 8:14:49 PM. This article is licensed under a Creative Commons Attribution-NonCommercial 3.0 Unported Licence.

where SBD corresponds to bulk density (g cm^{-3}), D_{sw}: dry soil weight (g), Vol_c: volume of the sampling cylinder (cm^3).

2.5 Species identification and richness

In all plots studied ($n = 12$) across the three tropical dry forest (TDF) subtypes, a thorough plant identification process was carried out, focusing primarily on trees and some shrubs. Other plant groups—such as graminoids, small herbaceous species, climbing plants, and very small seedlings—were not systematically recorded, as these life forms are typically not considered in forest carbon stock assessments due to their relatively low biomass contribution. To ensure accurate identification, plant individuals were marked with plastic tags labelled with unique codes, both during the dry and rainy seasons. This method allowed for precise tracking of individual plants over time, providing valuable data on species persistence, growth, and seasonal variations in the forest subtypes. The identification process involved the use of taxonomic guides and the expertise of a botanist from the Botanical Garden of the Universidad Técnica de Manabí, Ecuador.

2.6 Determination of carbon in the components of the evaluated forests

The determination of carbon was assessed in three main ecosystem components: aboveground biomass carbon (CAGB), litterfall carbon (C-litterfall), and soil organic carbon (SOC). CAGB reflects the carbon stored in living plants, estimated through allometric equations. C-Litterfall accounts for the carbon in dead plant material that falls to the forest floor, contributing to nutrient cycling and carbon turnover. SOC represents the long-term storage of carbon in the soil, primarily from decomposed organic matter. Together, these components offer insights into the forest's carbon storage, cycling, and overall ecological balance, helping to understand the role of these forests in the global carbon cycle.

2.6.1 Aboveground biomass and plant carbon (CAGB). Aboveground biomass (AGB) for trees and shrubs was estimated in each plot, by determining the plant carbon content using allometric equations. Measurements of aboveground biomass were performed twice, once during the rainy period and once during the dry period.

The AGB and carbon storage were assessed semi-annually. To quantify the biomass and carbon storage in trees, an indirect method based on allometric equations developed by Chave[50] for TDFs was employed. The height was measured using a Suunto brand clinometer model PM-5/3760, and a 50 meter Truper brand measuring tape. The diameter at breast height (DBH) of the trees was measured using a 5 meter diametric tape (Forestry Suppliers). This procedure was applied only for trees and large shrubs with DBH $\geq$ 5 cm (smaller life forms such as herbaceous plants, seedlings, and lianas were not included). The density of each plant species was determined using the "Global Wood Density Database".[51] If a species was not present in the database, the density of the corresponding genus or family was used. To determine AGB, eqn (2) was applied:

$$\begin{aligned} AGB_{est} &= \exp(-2.187 + 0.916 \times \ln(\rho D^2 H)) \\ &= 0.112 \times (\rho D^2 H)^{0.916} \end{aligned} \quad (2)$$

where AGB_{est} corresponds to aboveground biomass (kg per tree), ρ is the wood density (g cm^{-3}), D is the diameter at breast height (cm), and H is the height (m).

After calculating AGB_{est}, the total aboveground biomass was calculated by multiplying the value obtained per plot by the conversion factor based on the plot size (100 m^2) eqn (3).

$$TAGB = \left(\frac{\sum AGB_{est}}{1000}\right) \times \left(\frac{10\,000}{\text{plot area}}\right) \quad (3)$$

Here TAGB is the total aboveground biomass (Mg ha^{-1}), $\sum AGB_{est}$ is the sum of the aboveground biomass of all trees in the plot (kg), the factor 1000 converts sample units from kg to Mg, and the factor 10 000 converts area from m^2 to hectares (ha).

The conversion from TAGB to carbon (CAGB) was calculated following the guidelines stipulated by the IPCC in the Good Practice Guidance for Land Use, Land-Use Change, and Forestry by using eqn (4):[52]

$$CAGB = (TAGB \times FC) \quad (4)$$

where CAGB corresponds to carbon in aboveground biomass (Mg ha^{-1}), TAGB is the total aboveground biomass, FC is the carbon fraction, with a standard value of 0.50.

2.6.2 Litterfall carbon (C-litterfall). Three homemade litterfall traps, each with a surface area of 1 m^2 and a 1 mm mesh net for efficiency, were placed under randomly trees in each plot of the TDF subtypes. A total of three traps per plot were installed, with 36 traps used for both the rainy and dry campaigns. To assess litterfall carbon inputs, we installed the three litterfall traps within each 10 × 10 m plot. To ensure unbiased sampling and adequately capture spatial heterogeneity in litter deposition, we implemented a randomized placement strategy. Specifically, a 2 × 2 m grid was overlaid on each plot, generating 25 equally sized cells. Using a random number generator, we selected three cells per plot, and each litterfall trap was positioned at the center of a selected cell. The same traps were positioned 80 cm above the ground throughout both periods. Litterfall was collected monthly during two distinct periods: (a) March to May, representing the rainy period ($n = 3$), and (b) September to November, representing the dry period ($n = 3$).

The litter leaves collected in the field were placed in paper bags for transportation to the Laboratory of Agroecosystems and Climate Change (FAGROCLIM) at the Universidad Técnica de Manabí (Ecuador). Upon arrival, the fresh litterfall biomass was measured using an analytical balance. The fresh litterfall was then oven-dried at 70 °C for 48 hours. Finally, the dried leaves were weighed using an analytical balance to determine the dry litterfall biomass. Litterfall production was determined using eqn (5).[53]

$$P = \frac{\text{total dry weight (g)} \times 10^8\ \text{cm}^2 \times 30\ \text{days} \times 1\ \text{Mg}}{\text{area (10 000 cm}^2) \times \text{time (30 days)} \times 1\ \text{ha} \times 1\ \text{month} \times 10^6} \quad (5)$$

Open Access Article. Published on 15 August 2025. Downloaded on 2/27/2026 8:14:49 PM. This article is licensed under a Creative Commons Attribution-NonCommercial 3.0 Unported Licence.

where P corresponds to litterfall production (Mg ha^{-1}).

The conversion from litterfall to carbon (C-litterfall) was calculated following the guidelines stipulated by the IPCC in the Good Practice Guidance for Land Use, Land-Use Change, and Forestry by using eqn (4) mentioned above.[52]

2.6.3 Soil organic carbon. SOC was determined using the Walkley–Black method,[54] a volumetric technique based on chromium (Cr) oxidation. Briefly, 5 g of oven-dried soil was treated with 10 mL of 1 N potassium dichromate ($K_2Cr_2O_7$) solution, followed by 20 mL of concentrated sulfuric acid (H_2SO_4). The excess dichromate was titrated with 0.5 N ammonium iron(II) sulfate hexahydrate [$Fe(SO_4)_2 \cdot 6H_2O$] solution. Calculations were performed using eqn (6).

$$\text{SOC } (\%) = \frac{(v_{\text{blank}} - v_{\text{sample}}) \times M_{F_2} \times 0.003 \times 100 \times f \times mcf}{\text{W}} \tag{6}$$

where SOC (%) is the percentage of soil organic carbon (%); v_{blank} is the volume of titrant used in the blank (ml); v_{sample} is the volume of titrant used in the sample (ml); M_{F_2} is the molarity of standardized solution of Fe $(SO_4)_2 \cdot 6H_2O$; f is the correction factor 1.3; mcf is the correction factor for humidity (1.724); and W is the weight of soil (g). For the determination of soil organic carbon, eqn (7) was used.[55]

$$\text{SOC} = \text{SOC\%} \times \text{SBD} \times S_{\text{d}} \tag{7}$$

where SOC corresponds to soil organic carbon (Mg ha^{-1}), SOC% is the percentage of soil organic carbon, SBD is the bulk density (g cm^{-3}), and S_{d} is the soil depth (m). Carbon storage in forests was determined by averaging the values from the two soil depths and adding the allometric tree carbon and the carbon obtained from litterfall (eqn (8)).

$$\text{Carbon storage} = \text{SOC} + \text{CAGB} + P \tag{8}$$

2.7 Carbon extrapolation and stock estimation

To estimate total carbon stocks across the three forest subtypes—low-statured forest (LSF), short palm forest (SPF), and low dense forest (LDF)—we quantified carbon in three major pools: soil organic carbon (SOC), litterfall carbon (C-litterfall), and aboveground biomass carbon (CAGB). For each plot, carbon stock values were calculated per pool and expressed in megagrams of carbon per hectare (Mg C ha^{-1}). The values obtained for both climatic periods (rainy and dry) were averaged by forest subtype to produce a representative carbon stock per hectare.

Extrapolation to the landscape level was performed using a direct arithmetic approach. Specifically, the mean carbon stock per hectare for each forest subtype was multiplied by the total area (in hectares) occupied by that subtype, based on mapped forest patches. This yielded the total extrapolated carbon stock in Mg C for each forest type. No statistical model or inferential method was applied in this calculation. This method provides a transparent, area-weighted scaling of empirical carbon data suitable for comparative ecological assessments.

2.8 Statistical analyses

Statistical analyses were performed using R programming language (version 4.2.3) within the RStudio environment.[56] The Shapiro–Wilk test was applied to assess data normality, while the Levene test was used to evaluate the homogeneity of variances. Species richness (number of species) and abundance across plots, forest subtypes, and climatic periods were analyzed using PAST version 4.15.[57]

An analysis of variance (ANOVA) was conducted to compare the means of soil organic carbon (SOC), aboveground biomass carbon (CAGB), and carbon from litterfall (C-litterfall) among forest subtypes to identify statistically significant differences. Bar graphs were generated to visualize the distributions of SOC, CAGB, and C-litterfall across the analyzed factors (plots, forest subtypes, depths, and climatic periods). Boxplots to monitor monthly and three-month averages of C-litterfall were also produced using R. C-Litterfall *post hoc* Fisher tests ($P < 0.05$) were performed using Minitab version 21.1.0 to further explore group differences. For comparisons between soil depths and climatic periods, Student's t-tests ($P < 0.05$) were performed.

For SOC trends, two approaches were employed: (a) generating bar graphs for the two soil depths (0–40 cm and 40–80 cm) separately, and (b) calculating depth-weighted mean SOC values to produce a single bar representing the 0–80 cm soil depth. For litterfall analysis, two proxies were applied: (a) monthly mean litterfall biomass was plotted separately for three months, and (b) an average litterfall biomass was calculated over the same three-month period.

The total carbon stock was determined by summing the contributions of SOC, CAGB, and carbon from litterfall for each forest subtype and climatic period. These values were then used to estimate the total annual carbon stock and extrapolated to represent the carbon storage capacity of each forest subtype.

3 Results and discussion

3.1 Physical and chemical soil properties

The physical and chemical variables quantified in the soil showed different patterns across soil depths, climatic periods, and forest subtypes. These differences may be attributed to a variety of factors influencing soil conditions (Table 2).[58,59]

The differences in the physico-chemical properties of the soil may be linked to several factors like vegetation structure and composition, topography, climate, weathering processes and microbial activity and several other biotic and abiotic factors. In the highly dissected landscapes, bioclimatic conditions change rapidly and may vary over short distances, resulting in pronounced heterogeneity of soil types and their chemical and physical properties, hence influencing the vegetation and litter types as well as plant productivity which may affect the overall constitution of the ecosystem.[60–64]

The soil properties measured across the three tropical dry forest (TDF) subtypes—Jama-Zapotillo Lowland Semideciduous

 © 2025 The Author(s). Published by the Royal Society of Chemistry

Open Access Article. Published on 15 August 2025. Downloaded on 2/27/2026 8:14:49 PM.
This article is licensed under a Creative Commons Attribution-NonCommercial 3.0 Unported Licence.

Table 2 Soil properties by forest subtypes and climatic periods. LSF: Jama-Zapotillo Lowland Semideciduous Forest; SPF: Deciduous Pacific Forest of the Equatorial Coast; LDF: Lowland Deciduous Forest and Shrubland of Jama-Zapotillo. EC: electrical conductivity; SBD: bulk density; D1: soil depth 0–40 cm; D2: soil depth 40–80 cm

		Soil properties		
Soil depth (cm)	Forest subtype	EC (μS cm^{-1})	pH	SBD (g cm^{-3})
Rainy period				
	LSF	190.85 ± 24.25	7.93 ± 0.14	1.04 ± 0.06
D1: 0–40	SPF	148.98 ± 26.41	7.94 ± 0.23	0.92 ± 0.06
	LDF	151.82 ± 25.59	7.53 ± 0.25	0.89 ± 0.02
	LSF	196.85 ± 31.17	8.04 ± 0.18	1.04 ± 0.08
D2: 40–80	SPF	152.02 ± 14.22	7.89 ± 0.23	0.94 ± 0.08
	LDF	181.83 ± 14.22	7.63 ± 0.23	0.90 ± 0.05
Dry period				
	LSF	204.00 ± 54.89	6.84 ± 0.36	0.91 ± 0.09
D1: 0–40	SPF	183.75 ± 26.41	7.64 ± 0.23	1.00 ± 0.02
	LDF	190.28 ± 39.35	7.51 ± 0.19	0.88 ± 0.01
	LSF	181.94 ± 26.10	7.07 ± 0.41	0.91 ± 0.07
D2: 40–80	SPF	172.64 ± 14.22	7.78 ± 0.23	1.02 ± 0.02
	LDF	186.45 ± 52.99	7.21 ± 0.64	1.90 0.01

Forest (LSF), Deciduous Pacific Forest of the Equatorial Coast (SPF), and Lowland Deciduous Forest and Shrubland of Jama-Zapotillo (LDF) show distinct patterns that reflect the climatic conditions and edaphic diversity of the region.[58]

Regarding pH, no significant changes were observed at different soil depths, but substantial variation was noted between climatic periods (SI 2). During the dry period, soil acidification occurred due to reduced moisture, which led to the concentration of minerals and a lowering of the pH.[65] This acidification was particularly pronounced in LSF, where the decomposition of litterfall produced organic acids, further increasing soil acidity.[66,67] This result aligns with findings in other TDFs, where organic acid production during dry periods contributes to increased soil acidity. Conversely, during the rainy period, soils in SPF had lower pH values, likely driven by increased water availability and organic matter decomposition. These findings are consistent with studies suggesting that moisture availability and the decomposition of organic matter have a strong influence on soil pH dynamics.[68,69]

Soil electrical conductivity (EC) remained relatively constant across depths and subtypes during the dry period, but significant differences were observed during the rainy period (SI 2). These variations are influenced by precipitation rates, which affect the concentration of salts and minerals in the soil. During the rainy period, higher rainfall leads to leaching, which can reduce mineral concentrations, whereas under drier conditions, salts may accumulate. This variation is consistent with previous studies linking precipitation to changes in soil salinity.[68,70–72]

Soil bulk density (SBD) exhibited similar stability to conductivity, with no significant variation between soil depths (SI 2), but notable differences across forest subtypes and climatic periods. The observed variation in SBD could be attributed to differences in soil texture, as the geological composition remains constant across depths but can vary between climatic periods and forest subtypes.[73,74] Some soils are more prone to compaction under dry or wet conditions, depending on their clay, silt, and sand content. These results indicate that soil texture plays a key role in how moisture influences soil structure, and it is critical for understanding soil compaction dynamics under varying climatic conditions.[75,76]

Our pH values (ranging from 6.8 to 8.0) are consistent with those reported in TDFs in Florida and Loja province, Ecuador, which range from 6 to 8.1.[77,78] However, they are slightly higher than those found in Brazil's Caatinga (5.4 to 6.5)[79] and India's TDFs (5.9 to 6.4).[80] EC values in our study (ranging from 149.0 to 204.0 μS cm^{-1}) surpass those reported in Indian forests (120–140 μS cm^{-1})[81] but are consistent with those observed in Peruvian forests (162–210 μS cm^{-1}).[82] These findings highlight the unique edaphic conditions of the Ecuadorian coast, with its specific combination of temperature, precipitation, and forest type influencing soil properties.

3.2 Plant species identity and richness

A total of 47 plant species were identified across the forest subtypes examined in this study (Table 3).[83,84] Among these, the Jama-Zapotillo Lowland Semideciduous Forest (LSF) exhibited the highest species richness, with 25 species. This was followed by the Lowland Deciduous Forest and Shrubland of Jama-Zapotillo (LDF), which contained 19 species, and the Deciduous Pacific Forest of the Equatorial Coast (SPF), which had 18 species. Each forest subtype demonstrated a unique species composition, indicative of ecological specialization. The LSF contained 18 unique species, while the LDF and SPF hosted 10 and 9 unique species, respectively (more details available in SI 3–SI 8). Notably, only three species were classified as cosmopolitan, occurring in all three subtypes. This low number of cosmopolitan species reflects the influence of distinct environmental and edaphic factors, such as humidity, altitude, precipitation, temperature, and soil properties on plant species distribution and ecological specialization within these forests.

Open Access Article. Published on 15 August 2025. Downloaded on 2/27/2026 8:14:49 PM.
This article is licensed under a Creative Commons Attribution-NonCommercial 3.0 Unported Licence.

Table 3 Identified plant species in the three tropical dry forest (TDF) subtypes over a year: LSF (Jama-Zapotillo Lowland Semideciduous Forest); SPF (Deciduous Pacific Forest of the Equatorial Coast); and LDF (Lowland Deciduous Forest and Shrubland of Jama-Zapotillo). Plant species in bold represent cosmopolitan species present in all forest subtypes

			Forest subtypes		
No.	Plant specie	Family	LSF	SPF	LDF
1	*Cordia hebeclada*	Cordiaceae		—	—
2	*Zanthoxylum fagara*	Rutaceae			—
3	*Clavija pungens*	Primulaceae			—
4	*Delostoma integrifolium*	Bignoniaceae		—	—
5	*Ziziphus thyrsiflora*	Rhamnaceae		—	
6	*Guazuma ulmifolia*	Malvaceae		—	—
7	*Piptadenia flava*	Fabaceae		—	—
8	*Trema integerrima*	Cannabaceae		—	—
9	***Croton fraseri***	Euphorbiaceae			
10	*Serjania caracasana*	Sapindaceae		—	—
11	*Amphilophium paniculatum*	Bignoniaceae		—	—
12	*Sesbania herbacea*	Fabaceae		—	—
13	*Ximenia americana*	Ximenaceae		—	—
14	*Pseudosamanea guachapele*	Fabaceae		—	—
15	*Leucaena trichodes*	Fabaceae		—	
16	*Handroanthus chrysanthus*	Bignoniaceae		—	—
17	*Cordia macrantha*	Lauraceae		—	—
18	*Piper sanctum*	Piperaceae		—	—
19	***Croton eggersii***	Euphorbiaceae			
20	*Acnistus arborescens*	Solanaceae		—	—
21	***Zanthoxylum sprucei***	Rutaceae			
22	*Samanea saman*	Fabaceae		—	—
23	*Erythrina poeppigiana*	Fabaceae		—	—
24	*Randia armata*	Rubiaceae		—	—
25	*Triumfetta althaeoides*	Malvaceae		—	—
26	*Melampodium divaricatum*	Asteraceae	—		
27	*Cordia macrocephala*	Cordiaceae	—		—
28	*Pithecellobium arboreum*	Fabaceae	—		—
29	*Senna oxyphylla*	Fabaceae	—		
30	*Cordia lutea*	Cordiaceae	—		
31	*Bonellia sprucei*	Primulaceae	—		—
32	*Crateva Sp*	Crateva	—		—
33	*Trema micrantha*	Cannabaceae	—		—
34	*Hilleria secunda*	Petiveriaceae	—		—
35	*Achatocarpus pubescens*	Achatocarpaceae	—		—
36	*Malpighia glabra*	Malpighiaceae	—		—
37	*Condylidium iresinoides*	Asteraceae	—		—
38	*Phyllanthus amarus*	Phyllanthaceae	—	—	
39	*Varronia curassavica*	Cordiaceae	—	—	
40	*Tournefortia hirsutissima*	Heliotropiaceae	—	—	
41	*Cynophalla heterophylla*	Capparaceae	—	—	
42	*Cynophalla flexuosa*	Capparaceae	—	—	
43	*Agonandra silvatica*	Opiliaceae	—	—	
44	*Caryocar glabrum*	Caryocaraceae	—	—	
45	*Caesalpinia tinctoria*	Fabaceae	—	—	
46	*Libidibia glabrata*	Fabaceae	—	—	
47	*Vallesia glabra*	Apocynaceae	—	—	

3.3 Carbon fluctuations in the three tropical dry forest subtypes

3.3.1 Plant biomass carbon among tropical dry forests. The carbon storage potential, measured as CAGB, varied among forest subtypes under different climatic conditions, but no significant differences were observed between the rainy and dry seasons (Table 4, Fig. 3).

In the LSF, CAGB was 27.4 Mg ha^{-1} during the rainy period and increased slightly in the dry periods. The annual average carbon contribution for this forest subtype was 28.8 Mg ha^{-1}. The carbon contribution of specific species within this subtype was significant, with *Trema integerrima* and *Pseudosamanea guachapele* being the highest contributor.

The SPF had lower overall carbon contributions during the rainy and the dry periods (Table 4). Its annual average carbon contribution was 13.0 Mg ha^{-1}. Among the species in this forest subtype, *Croton eggersii*, and *Cordia macrocephala* were the most important contributors.

The LDF exhibited the highest values during both the rainy and dry periods with an annual carbon contribution of 37.4 Mg ha^{-1}. Species such as *Cordia lutea*, *Tournefortia hirsutissima*, and *Ziziphus thyrsiflora* were notable contributors.

Analysis of the total carbon contribution of species and individuals across the forest subtypes (Fig. 3, SI 9 to SI 11) revealed that only a limited subset met the criteria necessary for quantification using allometric equations. Specifically, 9 species comprising 33 individuals in the LSF, 7 species with 55 individuals in the SPF, and 14 species encompassing 82 individuals in the LDF fulfilled the requirements for this analysis. This finding highlights the restricted pool of species within these subtypes that contribute directly to the assessment of plant biomass carbon, emphasizing the importance of species selection in accurately estimating carbon dynamics within these ecosystems.

These carbon production trends can be attributed to the moderate growth in tree diameter and height typically observed in TDFs. Consequently, arboreal biomass remains relatively stable throughout the year[85,86] (SI 13). Across the study sites, a clear gradient in allometric carbon production was evident.

In the LSF, species such as *Leucaena trichodes*, *Cordia macrantha*, and *Trema integerrima* exhibit notably tall stems (30–50 meters) and large diameters (up to 1 meter), contributing to higher CAGB. In contrast, the SPF and LDF, which experience lower precipitation rates, are dominated by smaller trees with reduced diameters, such as *Cordia lutea* and *Tournefortia hirsutissima*. Variations in the structural composition of vegetation directly influence the capacity of plants to absorb and store carbon, resulting in differences in carbon dynamics observed across these forest subtypes.[75–77] Other factors, such as forest fragmentation, microclimatic conditions, and soil quality, can further influence allometric carbon production.[90,91] Additionally, human-induced environmental changes can significantly impact the carbon dynamics of forests.

In general, the aboveground biomass values observed in this study align well with those reported for similar TDFs. The values recorded in the LDF are consistent with those documented for other TDFs in Ecuador and the Yucatán region of Mexico, ranging from 34.7 to 63.8 Mg ha^{-1}.[67,92] Similarly, the biomass values observed in the LSF are comparable to those reported for TDFs in Brazil and Tanzania, with an average of 27.5 Mg ha^{-1}.[93,94] In the SPF, biomass values resemble those found in the Brazilian Caatinga, approximately 14.2 Mg ha^{-1},[90,95] and

 © 2025 The Author(s). Published by the Royal Society of Chemistry

Open Access Article. Published on 15 August 2025. Downloaded on 2/27/2026 8:14:49 PM.
This article is licensed under a Creative Commons Attribution-NonCommercial 3.0 Unported Licence.

Table 4 Carbon aboveground biomass contribution ($n = 23$) in the three TDF forest subtypes. LSF: The Jama-Zapotillo Lowland Semideciduous Forest; SPF: Deciduous Pacific Forest of the equatorial coast; and LDF: Lowland Deciduous Forest and Shrubland of Jama-Zapotillo. Letters at the end of each forest subtype acronym indicate the climatic period as follows: rainy (R) and dry (D)

		Plant species carbon contribution (Mg ha^{-1})					
#	Plant species	LSF-R	LSF-D	SPF-R	SPF-D	LDF-R	LDF-D
1	*Cynophalla heterophylla*	—	—	—	—	1.70	1.76
2	*Varronia curassavica*	—	—	—	—	1.39	1.40
3	*Phyllanthus amarus*	—	—	—	—	1.00	1.05
4	*Tournefortia hirsutissima*	—	—	—	—	6.70	6.83
5	*Cordia lutea*	—	—	2.15	2.27	13.76	13.86
6	*Cynophalla flexuosa*	—	—	—	—	0.31	0.31
7	*Leucaena trichodes*	5.52	7.06	—	—	0.25	0.29
8	*Zanthoxylum sprucei*	—	—	0.19	0.20	1.61	1.64
9	*Croton eggersii*	—	—	4.48	4.40	0.10	0.11
10	*Croton fraseri*	0.11	0.14	—	—	2.92	2.98
11	*Ziziphus thyrsiflora*	—	—	—	—	5.41	5.48
12	*Melampodium divaricatum*	—	—	0.18	0.21	0.31	0.32
13	*Agonandra sylvatica*	—	—	—	—	1.20	1.20
14	*Pithecellobium arboretum*	—	—	3.45	3.58	0.42	0.44
15	*Bonellia sprucei*	—	—	0.92	0.96	—	—
16	*Cordia macrocephala*	—	—	1.42	1.51	—	—
17	*Trema integerrima*	6.35	6.65	—	—	—	—
18	*Pseudosamanea guachapele*	4.87	5.00	—	—	—	—
19	*Cordia macrantha*	4.14	4.25	—	—	—	—
20	*Ximenia americana*	4.28	4.51	—	—	—	—
21	*Sesbania herbacea*	1.42	1.65	—	—	—	—
22	*Acnistus arborescens*	0.17	0.18	—	—	—	—
23	*Guazuma ulmifolia*	0.53	0.72	—	—	—	—
	Total by climatic period	27.40	30.17	12.78	13.12	37.08	37.66
	Total by forest type	28.79 ± 1.96		12.95 ± 0.24		37.37 ± 0.41	

even exceed the values recorded in Caicó, Brazil, where biomass levels were as low as 8.9 Mg ha^{-1}.[96]

The PCA biplot in Fig. 4, provides a clear visualization of the variability in CAGB contributions among plant species across the three TDF subtypes. Together, the first two principal components explain 85.71% of the total variability, with PC1 accounting for 46.05% and PC2 for 39.66%. This high percentage indicates that most of the variability in species

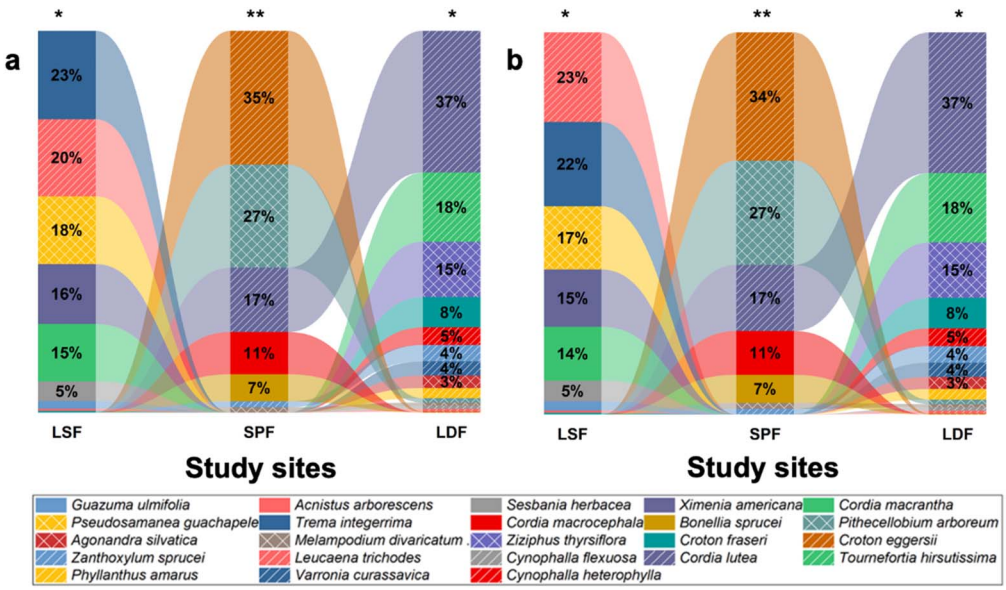

Fig. 3 Carbon contribution (%) of main plant species by sites and climatic periods. LSF: Jama-Zapotillo Lowland Semideciduous Forest; SPF: Deciduous Pacific Forest of the Equatorial Coast; LDF: Lowland Deciduous Forest and Shrubland of Jama-Zapotillo. (a) Rainy period; (b): dry period. Different numbers of asterisks indicate statistically significant differences between sites ($P < 0.05$).

Open Access Article. Published on 15 August 2025. Downloaded on 2/27/2026 8:14:49 PM.
This article is licensed under a Creative Commons Attribution-NonCommercial 3.0 Unported Licence.

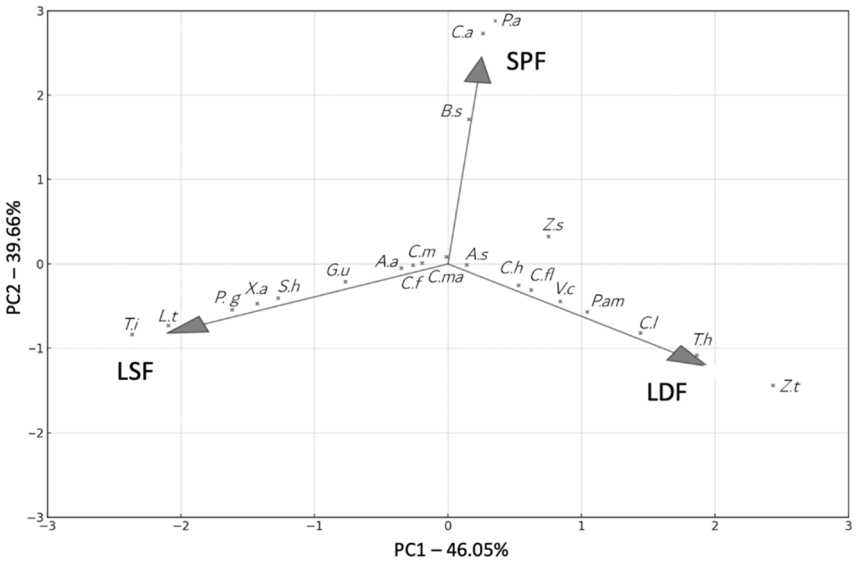

Fig. 4 Principal component analysis of variability in CAGB contributions among plant species across the three TDF subtypes. LSF: Jama-Zapotillo Lowland Semideciduous Forest; SPF: Deciduous Pacific Forest of the Equatorial Coast; and LDF: Lowland Deciduous Forest and Shrubland of Jama-Zapotillo. *T.i*: *Trema integérrima*, *P.g*: *Pseudomanea guachapele*, *C.ma*: *Cordia macrantha*, *X.a*: *Ximenia americana*, *S.h*: *Sesbania herbácea*, *C.f*: *Croton fraseri*, *A.a*: *Acnistus arborescens*,*G.u*: *Guazuma ulmifolia*, *L.t*: *Leucaena trichodes*, *C.e*: *Croton eggersii*, *B.s*: *Bonellia sprucei*, *Z.s*: *Zanthoxylum sprucei*, *P.a*: *Pithecellobium arboreum*, *C.l*: *Cordia lutea*, *M.d*: *Melampodium divaricatum*, *C.m*: *Cordia macrocephala*, *C.h*: *Cynophalla heterophylla*, *V.c*: *Varronia curassavica*, *P.am*: *Phyllanthus amarus*, *T.h*: *Tournefortia hirsutissima*, *C.f*: *Cynophalla flexuosa*, *A.s*: *Agonandra silvatica*, and *Z.t*: *Ziziphus thyrsiflora*.

contributions to carbon stocks across these subtypes is well represented. The plot reveals strong differentiation among the forest subtypes, as indicated by the directions and lengths of the vectors, which reflect variability in species contributions and the ecological characteristics of each forest.

The LDF vector, extending strongly along the positive PC1 axis, underscores significant variability in CAGB contributions by its species. Dominant species associated with LDF, such as *Cordia lutea* (*C.l*), *Tournefortia hirsutissima* (*T.h*) and *Ziziphus thyrsiflora* (*Z.t*), are positioned far along PC1, suggesting their substantial contributions to biomass in this subtype. This pattern reflects the ecological adaptability of these species to the drier and more open conditions characteristic of LDF. In contrast, the SPF exhibited shorter vector pointing sharply upward along PC2, driven by species such as *Bonellia sprucei* (*B.s*), *Croton eggersii* (*C.e*) and *Pithecellobium arboretum* (*P.a*), which are prominently associated with high biomass.

Meanwhile, the LSF vector is positioned in the negative PC1 region, suggesting lower variability in species contributions to biomass. Species such as *Trema integerrima* (*T.i*), *Leucaena trichodes* (*L.t*), and *Pseudomanea guachapele* (*P.g*) are closely aligned with LSF, indicating a higher and more balanced distribution of carbon biomass contributions among these species. This stability may reflect the less fragmented and more consistent environmental conditions of LSF compared to the other forest subtypes. The clustering of species near the origin, such as *Cordia macrantha* (*C.ma*) and *Cynophalla heterophylla* (*C.h*), suggests shared contributions across multiple subtypes or relatively low variability in biomass contributions.

These patterns emphasize the ecological and functional differences between the TDF's subtypes in terms of species identity and carbon dynamics. The high variability in LDF reflects its transitional nature, with a mix of drought-tolerant shrubs and deciduous trees that dominate its carbon storage potential. The SPF, on the other hand, demonstrates pronounced species dominance, highlighting its adaptation to seasonal drought and coastal influences. In contrast, the LSF presents a more uniform distribution of species contributions to biomass, reflecting its relatively stable ecosystem and less extreme environmental variability.[97,98] These findings underscore the importance of considering species-specific contributions and forest subtype characteristics when assessing carbon dynamics and ecosystem functioning in TDFs.

3.3.2 Litterfall carbon among tropical dry forests. The amount of allometric carbon is directly related to plant species identity present in the forests, rather than to the number of individuals. However, the variation in the amount of carbon in litterfall differs significantly between climatic periods[99,100] (Fig. 5A, B; SI 12 and 13).

In the monthly C-litterfall analysis (Fig. 5A), the LSF showed, on average, the highest contribution during both periods (rainy and dry), with values ranging from 0.18 Mg ha^{-1} (rainy) to 0.59 Mg ha^{-1} (dry). In contrast, the SPF and LDF exhibited very similar monthly C-litterfall values, varying from 0.04 Mg ha^{-1} (SPF, dry) to 0.11 Mg ha^{-1} (SPF, rainy).

Values of three-month average C-litterfall in the LSF were found to be higher during the dry period (0.57 Mg ha^{-1}) than during the rainy period (0.21 Mg ha^{-1}) (Fig. 5B). This result is consistent with other studies,[85–87] indicating an inverse relationship between leaf fall and the precipitation rate in forests with large trees.[88,89] These trees often have mechanisms to cope with low water levels, such as shedding leaves to reduce water

 © 2025 The Author(s). Published by the Royal Society of Chemistry

Open Access Article. Published on 15 August 2025. Downloaded on 2/27/2026 8:14:49 PM.
This article is licensed under a Creative Commons Attribution-NonCommercial 3.0 Unported Licence.

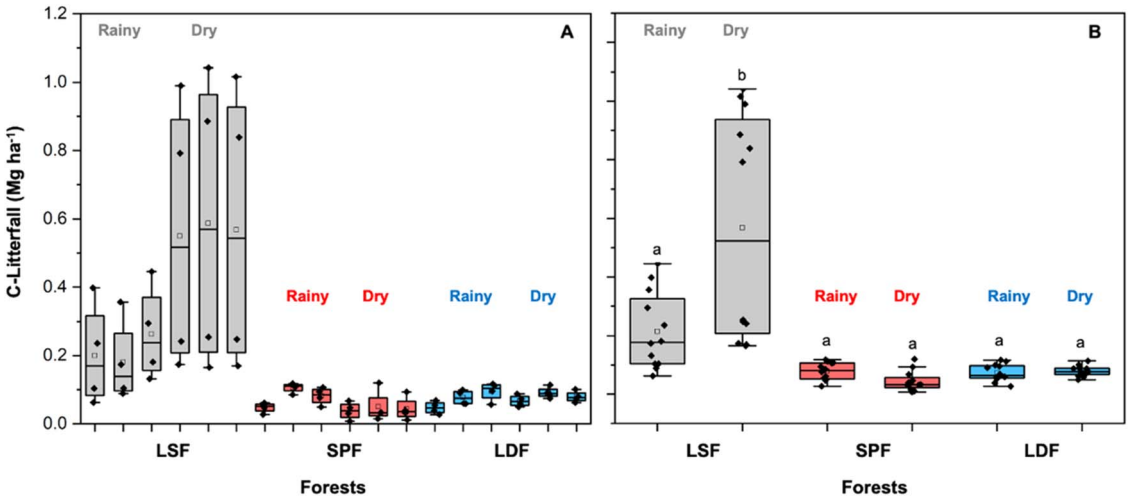

Fig. 5 Litterfall carbon across forests and climatic periods. (A): Monthly C-litterfall; (B): three-month average C-litterfall. LSF: Jama-Zapotillo Lowland Semideciduous Forest; SPF: Deciduous Pacific Forest of the Equatorial Coast; and LDF: Lowland Deciduous Forest and Shrubland of Jama-Zapotillo. Different lowercase letters indicate statistically significant differences between sites and climatic period interactions ($P < 0.05$).

loss through transpiration.[85–87] In the case of SPF and LDF, a decrease in the three-month average C-litterfall was observed compared to LSF. In SPF, values of 0.08 Mg ha^{-1} during the rainy period and 0.04 Mg ha^{-1} during the dry period, respectively, were recorded while in LDF, similar values of 0.08 Mg ha^{-1} in the dry period and 0.07 Mg ha^{-1} in the rainy period were observed.

When comparing the three-month average C-litterfall among forest subtypes, it was evident that the values did not show significant differences during the rainy period (Fig. 5B). However, in the dry period, there was a clear disparity, with the LSF value being considerably higher than those of the SPF and LDF forests, which presented very similar values. This is probably because the plant species present in these forests (SPF and LDF) do not have many leaves in their canopies, resulting in less variation between the stages.[101,102] It is noteworthy that a key factor in this disparity could be the severity of dryness during the dry period in each forest.

These contrasting patterns of C-litterfall among forest subtypes may be attributed to differences in forest structure, species composition, and local climatic conditions. In the LSF, the presence of taller trees with larger diameters and denser canopies, such as *Trema integerrima* and *Leucaena trichodes*, likely contributes to the more pronounced litterfall observed during the dry season. These species are known to shed leaves as a water-saving strategy during drought periods, a mechanism commonly reported in deciduous tropical dry forest.[103,104] Conversely, the SPF and LDF sites are structurally more open, with lower canopy heights and a greater proportion of shrub or semi-evergreen species, which exhibit slower and less synchronized leaf turnover across seasons. This aligns with previous studies indicating that in drier and more xeric TDFs, litter production may remain relatively constant due to limited foliar biomass and reduced seasonality in leaf phenology.[105] Additionally, higher temperatures and lower precipitation in SPF and LDF may further constrain primary productivity and litter accumulation, limiting the seasonal signal in litterfall carbon. Such findings underscore the role of vegetation traits and climatic gradients in shaping carbon cycling across TDF landscapes.

The average C-litterfall values found in the SPF and LDF sites show similarities with those reported in tropical forests in Brazil[106] and slightly higher than those recorded in forests in Mexico, Colombia, and Ethiopia.[99,106,107] As for the LSF, its reported values resemble those of dry tropical forests in Thailand.[108,109]

3.3.3 Soil organic carbon among tropical dry forests. The variability of soil organic carbon (SOC) stocks by depth and among plots across the three tropical dry forest subtypes could be observed in Fig. 6.

The results presented in Fig. 6 highlight clear differences in SOC stocks between soil depths (D1 and D2) and among individual plots within each forest subtype. Across all three forest subtypes, the upper soil layer (D1) consistently exhibits higher SOC values compared to the deeper layer (D2), demonstrating the predominant accumulation of organic carbon in surface soils.

In the LSF, SOC stocks in D1 (0–40 cm) are particularly high, with plots P1 and P4 reaching 85.7 Mg ha^{-1} and 67.7 Mg ha^{-1}, respectively. In contrast, SOC values in D2 (40–80 cm) remain slightly lower across all plots (except P4), indicating a pronounced vertical gradient of SOC in this forest subtype. This pattern could suggest that organic matter inputs, such as leaf litter and fine roots, primarily accumulate and are retained in the upper soil layers.[63,110,111] In the SPF, SOC stocks in D1 are generally lower compared to the LSF, ranging from 54.7 to 73.6 Mg ha^{-1}. SOC values in D2 are consistently lower than those observed in the LSF and LDF. For instance, plots P6 and P8 show a relatively smaller gap between D1 and D2 SOC stocks. For the LDF, SOC stocks in D1 consistently exceed 61 Mg ha^{-1} across all plots, with the highest value observed in P10 (74.5 Mg ha^{-1}). SOC stocks in D2 for the LDF are slightly higher than

Open Access Article. Published on 15 August 2025. Downloaded on 2/27/2026 8:14:49 PM.
This article is licensed under a Creative Commons Attribution-NonCommercial 3.0 Unported Licence.

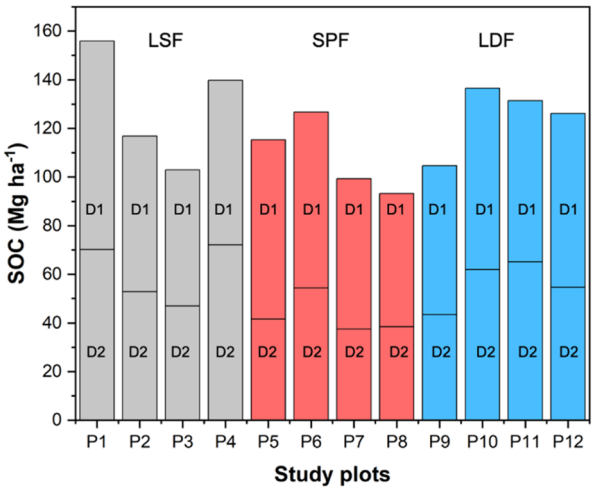

Fig. 6 Soil organic carbon across depths and plots. SOC: soil organic carbon; LSF: Jama-Zapotillo Lowland Semideciduous Forest; SPF: Deciduous Pacific Forest of the Equatorial Coast; LDF: Lowland Deciduous Forest and Shrubland of Jama-Zapotillo; Plots P1 to P4 belong to the LSF (bars in gray), P5 to P8 belong to the SPF (bars in red), and P9 to P12 belong to the LDF (bars in blue). D1: soil depth 0–40 cm; D2: soil depth 40–80 cm.

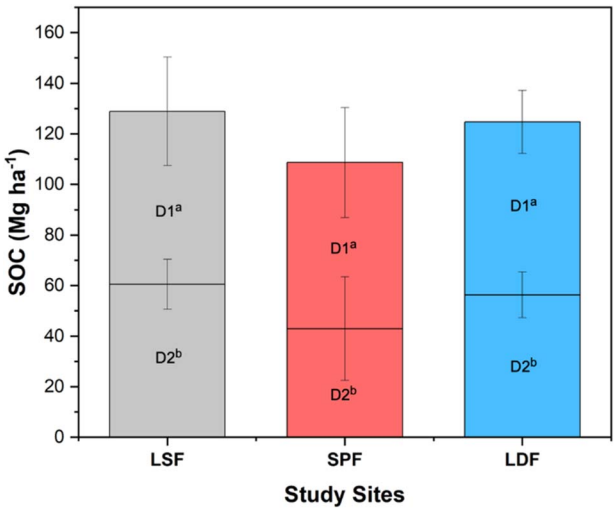

Fig. 7 Soil organic carbon by depth across forests subtypes (study sites). SOC: soil organic carbon; LSF: Jama-Zapotillo Lowland Semideciduous Forest; SPF: Deciduous Pacific Forest of the Equatorial Coast; LDF: Lowland Deciduous Forest and Shrubland of Jama-Zapotillo; D1: soil depth 0–40 cm; D2: soil depth 40–80 cm. Statistical differences between depths (D1 *vs.* D2) within each forest subtypes are indicated by lowercase letters.

those in the SPF but slightly lower than those in the LSF. Among the plots, the highest D2 value was recorded in P11 (65.1 Mg ha^{-1}), where SOC in D2 is nearly equivalent to D1, suggesting a more even vertical distribution.

Spatially, SOC stocks vary among plots within each forest subtype. The LSF and LDF exhibit the highest SOC concentrations in D1 across all subtypes, while the SPF generally shows slightly lower SOC stocks across both soil depths. These spatial and vertical differences in SOC storage likely reflect the combined effects of forest subtype-specific characteristics, local environmental factors, and plot-level variability in soil properties and plant dynamics.[112,113] In general, these findings suggest that deeper root systems or enhanced belowground processes, such as the transport or stabilization of organic matter in deeper horizons, may play a significant role in the carbon storage potential of these forest subtypes.[110]

Fig. 7 shows that SOC stocks in the upper layer (D1) are consistently higher than in the deeper layer (D2) across all forest subtypes. In the LSF, SOC in D1 reaches 68.4 Mg ha^{-1}, while D2 contributes 60.5 Mg ha^{-1}. In contrast, in the SPF, D1 SOC averages 65.6 Mg ha^{-1}, while D2 decreases to 43.0 Mg ha^{-1}. Similarly, in the LDF, SOC in D1 averages 68.4 Mg ha^{-1} compared to 56.3 Mg ha^{-1} in D2. Among the TDF subtypes, the largest variation in SOC between depths was observed in the SPF, with more than a 21% difference in D1. This pattern indicates that upper soil layers accumulate more carbon than deeper layers in all forest subtypes, although the magnitude of this difference varies.

Although the average SOC was higher in D1 (0–40 cm depth), the relative contribution of D2 to total SOC was significant, ranging from 40% in SPF to 45.2% in LDF, with the highest contribution observed in LSF at 47%. The greater contribution in LSF suggests that processes such as deeper root systems or slower carbon turnover may be more prominent in this forest subtype, emphasizing the importance of both vertical and spatial variability in SOC distribution.[111]

Fig. 8 presents SOC stocks (Mg ha^{-1}) for two soil depths (D1; D2) and climatic periods (rainy and dry).

During the rainy season, SOC in the upper soil layer (D1) is 80.6 Mg ha^{-1}, while the lower layer (D2) contains 75.6 Mg ha^{-1}, indicating a slight but significant difference between depths. In contrast, during the dry season, SOC in D1 decreases to 54.3 Mg ha^{-1}, and D2 drops to 44.0 Mg ha^{-1}, showing a more pronounced vertical variation. These findings suggest that the rainy period helps maintain relatively uniform SOC stocks between the upper and lower soil layers, whereas the dry period intensifies SOC stratification, with the upper layer (D1) retaining more carbon than the subsurface layer (D2). Climatic variations significantly influence SOC stocks, with both layers experiencing reductions from the rainy to the dry season.[114] During the dry season, SOC in the upper layer (D1) decreases by 32.6% compared to the rainy season, while D2 shows an even greater reduction of 41.9%. These findings highlight the sensitivity of SOC stocks to climatic conditions, particularly in the lower soil layer, which appears more vulnerable to moisture limitations during the dry period.[115]

These results reveal distinct patterns of SOC dynamics driven by depth and climatic periods. During the rainy season, SOC is relatively evenly distributed between D1 and D2, likely due to increased organic matter inputs, enhanced microbial activity, and the percolation of dissolved organic carbon to deeper soil layers under moist conditions.[58,116] However, during the dry period, SOC stocks are reduced at both depths, with the surface layer (D1) retaining more carbon than the lower layer (D2). This suggests that the surface layer benefits from its

 © 2025 The Author(s). Published by the Royal Society of Chemistry

Open Access Article. Published on 15 August 2025. Downloaded on 2/27/2026 8:14:49 PM.
This article is licensed under a Creative Commons Attribution-NonCommercial 3.0 Unported Licence.

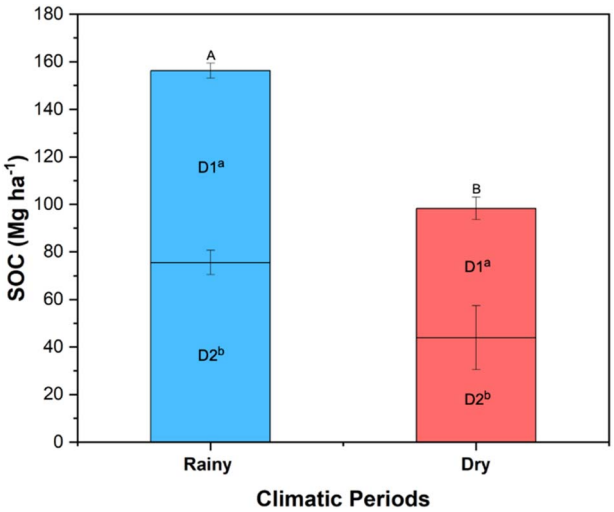

Fig. 8 Soil organic carbon by depth and climatic periods (rainy and dry). SOC: soil organic carbon; D1: soil depth 0–40 cm; D2: soil depth 40–80 cm. Statistical differences between depths (D1 *vs.* D2) within each climatic period are indicated by lowercase letters, while differences in total SOC between climatic periods are denoted by uppercase letters. Error bars represent standard deviations.

proximity to organic inputs, while the subsurface layer is more susceptible to carbon depletion when water availability is limited.[115]

These patterns underscore the importance of seasonal rainfall in maintaining SOC stocks in tropical dry forests. The pronounced reduction in SOC during the dry period, particularly at D2, indicates that prolonged droughts or shifts in rainfall regimes could disproportionately affect the subsurface soil, potentially leading to long-term carbon losses. Moreover, the observed vertical stratification during the dry period highlights the critical role of the surface layer in preserving SOC under moisture-limited conditions.

Seasonal differences in SOC stocks observed in Fig. 8 reflect the influence of climatic variability on soil carbon dynamics in tropical dry forests. Although SOC is generally considered a stable pool, emerging evidence suggests that short-term fluctuations are possible in response to seasonal shifts in soil moisture, organic inputs, and microbial activity.[117,118] During the rainy season, increased root exudation, litter decomposition, and microbial turnover likely contribute to higher SOC retention, whereas during the dry season, limited water availability may suppress microbial processes and accelerate SOC mineralization or redistribution.[119,120] These findings underscore the need to reconsider the assumption of SOC invariability over short timeframes, particularly in ecosystems with strong seasonality.

3.3.4 Carbon pool components in tropical dry forests. To compare the carbon pools across the three components (SOC, CAGB and C-litterfall) of tropical dry forests, a multi-level graphic (spatial and temporal) analysis was performed (Fig. 9).

Fig. 9A–C illustrate the depth-weighted average SOC distribution across sampling plots, forest subtypes, and climatic periods. SOC values exhibit considerable spatial variability across plots (Fig. 9A), ranging from 46.6 Mg ha^{-1} in P8 of SPF to over 78.0 Mg ha^{-1} in P1 of LSF. When compared across forest subtypes (Fig. 9B), LSF consistently has the highest SOC values (64.4 Mg ha^{-1}), followed by LDF (62.4 Mg ha^{-1}) and SPF (54.3 Mg ha^{-1}). While the SOC stocks (depth-weighted average) among forest subtypes show limited variability overall, significant statistical differences were observed between LSF and SPF. The ranking of SOC stocks by forest subtype is as follows: LSF > LDF > SPF, emphasizing the higher carbon storage capacity of LSF relative to the other forest types.

Regarding climatic periods (Fig. 9C), the depth-weighted average SOC is significantly higher during the rainy period (78.1 Mg ha^{-1}) compared to the dry periods (49.1 Mg ha^{-1}), highlighting the seasonal influence on soil carbon accumulation. Additionally, strong statistical differences in SOC were observed between these two climatic periods, further emphasizing the impact of seasonal variation (Fig. 9C).

The range of CAGB across sampling plots (Fig. 9D) is narrower compared to SOC, varying from less than 5.8 Mg ha^{-1} in some LDF plots (*e.g.*, P6) to over 58.2 Mg ha^{-1} in P10 of LSF. Forest comparisons (Fig. 9E) show that LDF has the highest CAGB (37.3 Mg ha^{-1}), followed by LSF (28.8 Mg ha^{-1}), while SPF exhibits significantly lower values (12.9 Mg ha^{-1}). In general, no significant differences in CAGB were found between LSF and LDF, while SPF showed markedly lower values compared to both forest types. Additionally, no significant variation in CAGB was observed between climatic periods (Fig. 9F), indicating that aboveground biomass carbon remains relatively stable across seasons.

The C-litterfall values (Fig. 9G) are considerably lower in magnitude compared to SOC and CAGB, ranging from 0.04 Mg ha^{-1} in SPF (P6) to 0.7 Mg ha^{-1} in LSF (P7). Forest comparisons (Fig. 9H) show that LSF has significantly higher litterfall carbon (0.4 Mg ha^{-1}) than both SPF (0.06 Mg ha^{-1}) and LDF (0.07 Mg ha^{-1}). Comparisons between climatic periods (Fig. 9I) suggest higher C-litterfall during the dry season, likely due to increased leaf shedding; however, these differences were not statistically significant.

3.5 Quantification of global carbon components across the three tropical dry forests

The results presented in Table 5 summarize differences in the distribution and dynamics of carbon pools (SOC, CAGB and C-litterfall) across the three TDF subtypes on the Ecuadorian coast.

The sum of total carbon stocks (by periods) varied significantly between climatic periods, highlighting the impact of seasonal changes on carbon dynamics (Table 5; SI 14 and SI15). LDF consistently exhibited higher carbon stocks, followed by LSF. In contrast, SPF had the lowest total carbon stocks.

The LSF and LDF appear to better buffer seasonal changes in carbon stocks, likely due to higher inputs of organic material, greater carbon stabilization mechanisms in the soil, or more robust vegetation cover. In contrast, the SPF's lower and more variable carbon stocks suggest that it is more vulnerable to the

Open Access Article. Published on 15 August 2025. Downloaded on 2/27/2026 8:14:49 PM.
This article is licensed under a Creative Commons Attribution-NonCommercial 3.0 Unported Licence.

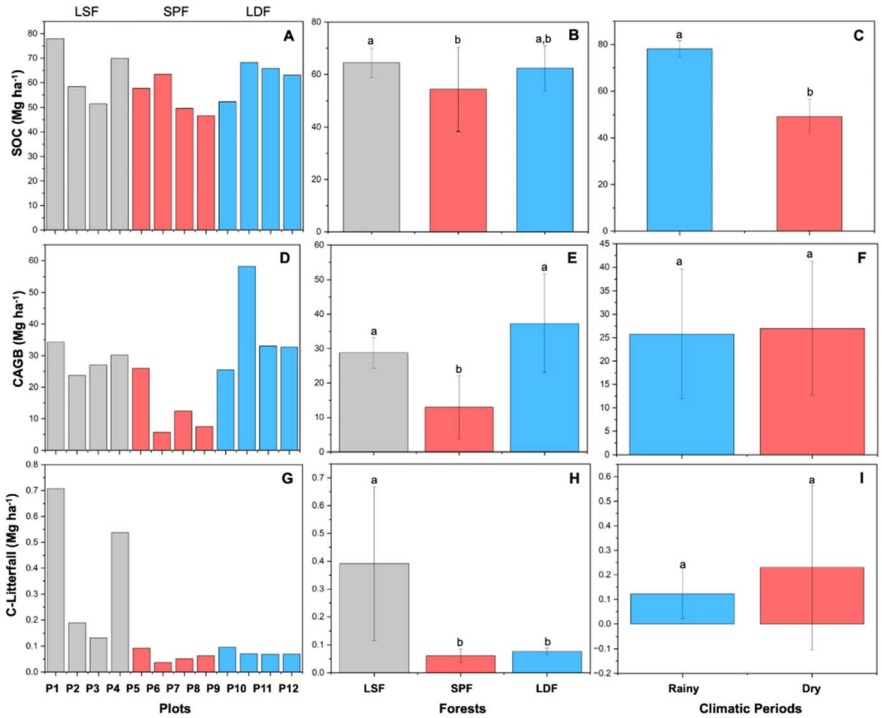

Fig. 9 Carbon pool trends across tropical dry forests. (A, D and G) Carbon pool variation across sampling plots; (B, E and H): carbon pool variation across forest subtypes; and (C, F and I): carbon pools across climatic periods. SOC: depth-weighted average (0–80 cm) of soil organic carbon ($n = 72$); CAGB: carbon aboveground biomass ($n = 12$); C-litterfall: 3 month-average of carbon litterfall ($n = 216$). LSF: Jama-Zapotillo Lowland Semideciduous Forest; SPF: Deciduous Pacific Forest of the Equatorial Coast; LDF: Lowland Deciduous Forest and Shrubland of Jama-Zapotillo. In (A, D and G), plots P1 to P4 belong to the LSF (bars in gray), P5 to P8 to the SPF (bars in red), and P9 to P12 to the LDF (bars in blue). Statistical differences between forests and climatic periods are indicated by lowercase letters ($P < 0.05$). Error bars represent standard deviations.

effects of climatic seasonality, potentially due to differences in forest structure, soil properties, or reduced carbon inputs.

The sum of total carbon by forest subtypes reveals the overall capacity of each forest subtype to store carbon on an annual basis. The LDF exhibited the highest total annual average carbon, followed by the LSF and the SPF. These averages further support the findings that the LDF and LSF are more carbon-dense forest subtypes, with the LSF maintaining substantial carbon stocks despite the seasonal fluctuations in litterfall and SOC.

The extrapolated total carbon stocks, calculated by multiplying the sum of total carbon for each forest subtype by the total forest patch area (as established by the Ministry of Environment, Water, and Ecological Transition of Ecuador)[46] highlight the significant role these forests play in regional carbon sequestration. The LDF, with the highest total carbon per patch, extrapolates to approximately 526 133.3 Mg, followed by the SPF with 463 133.0 Mg, and the LSF with 3113.3 Mg. The LDF, with the highest sum of total carbon per patch, extrapolates to approximately 526 133.3 Mg, followed by the SPF and LSF with

Table 5 Sum of total carbon stock across forest subtypes and climatic periods. Total carbon stock was estimated by summing three major components: aboveground biomass carbon (CAGB), litterfall carbon (litterfall-C), and soil organic carbon (SOC). For SOC, determinations were made at two soil depths: D1 (0–40 cm) and D2 (40–80 cm). These values were integrated by applying a depth-weighted average to account for differences in soil layer thickness. The total extrapolated carbon stocks was calculated by multiplying the sum of total carbon for each forest subtype by the total forest patch area. LSF: Jama-Zapotillo Lowland Semideciduous Forest; SPF: Deciduous Pacific Forest of the Equatorial Coast; LDF: Lowland Deciduous Forest and Shrubland of Jama-Zapotillo

	LSF		SPF		LDF	
Carbon quantification	Rainy	Dry	Rainy	Dry	Rainy	Dry
Sum of total carbon (Mg ha^{-1}) (climatic period)	103.34	84.66	82.21	52.59	107.24	92.52
Sum of total carbon (Mg ha^{-1}) (forest subtypes)	94.0		67.4		99.9	
Total extrapolated carbon of forest patches (Mg)	3113.3		463 133.0		526 133.3	

 © 2025 The Author(s). Published by the Royal Society of Chemistry

Open Access Article. Published on 15 August 2025. Downloaded on 2/27/2026 8:14:49 PM.
This article is licensed under a Creative Commons Attribution-NonCommercial 3.0 Unported Licence.

463 133.0 and 3113.3 Mg, respectively. These extrapolated estimates for the three TDF patches suggest that LDF and SPF have significant carbon storage capacities at the landscape scale. However, it is important to note that our study used the surface area of the specific patches where the plots are located. This means the total extrapolated carbon does not account for all patches of each forest subtype.

3.6 Implications and fragility of carbon storage potential

The carbon storage potential in the forests was determined by averaging the values from the two soil depths, summing the aboveground biomass carbon obtained from allometric equations and the carbon obtained from leaf litter. The highest amount of carbon in the forests was found in the soil, followed by aboveground biomass (allometric carbon) with the smallest amount of litterfall carbon. The total carbon stock was determined for each forest subtype, considering the average carbon storage potential between the rainy and dry periods to obtain an interpolated value representing the total carbon quantity at the forest subtypes.

The forest that showed the highest carbon storage potential was the LDF, closely followed by the LSF, and finally the SPF forest (Table 5). The carbon storage potential results at the study sites reveal significant variations. The values obtained exceed those reported in deciduous dry forests and dry shrub forests on the Ecuadorian coast,[67] and are similar to those reported in dry tropical forests in Madhya, India,[121] but lower than those reported in the dry tropical forests of Michoacán, Mexico.[122] These differences can be attributed to species diversity, as explained in previous paragraphs, the age of the forests, and climatic factors that have not been considered. Understanding these variations is crucial for designing strategies to combat climate change, conserve forests, and maximize carbon capture.

The importance of determining carbon stock at the study sites lies in understanding their potential as possible carbon sinks or sources. According to the literature, TDFs are currently considered highly fragile ecosystems, even more so than wetter ecosystems.[123] This is because they experience a severe increase in carbon losses, and their annual carbon gain rate is lower compared to the losses. This is largely attributed to rising temperatures, increased CO_2 levels, which lead to longer drought periods, affecting SOC, soil microorganisms, and plant species within these ecosystems.[123,124]

Although the carbon production from litterfall and aboveground biomass was higher during the dry period, carbon storage potential was greater during the rainy period. This is because the major portion of storage is determined by the SOC, which decreased during the dry period, directly affecting carbon storage potential. The carbon obtained from AGB is the most stable portion of carbon storage between climatic periods, as shown in this research; it may even persist over time,[85] unlike SOC, which varies between climatic periods. According to Pelletier,[125] high allometric carbon values play a crucial role in carbon sequestration and contribute to forests being considered sinks; in this case, the LSF and LDF subtypes would be favored as potential carbon sinks.

3.7 Study limitations and potential sources of bias

Despite the robust design of our study, which was validated in other ecosystems and temporal contexts, several limitations and potential sources of bias must be acknowledged. The inherent spatial heterogeneity of tropical dry forest soils suggests that larger sample sizes might be needed to fully capture true population parameters.[126] Although our sampling intensity followed established protocols, it may have been insufficient to characterize the fine-scale variability of these ecosystems.

One important limitation is the extrapolation of carbon stock estimates from a relatively small number of sampling plots per forest subtype ($n = 4$). While this small plot count provides an indicative measure of carbon stocks at the patch scale under standardized conditions, it is not intended to represent regional averages. Notably, there is no universally prescribed number of plots for tropical forest carbon assessments, and similar small-plot approaches have been employed in global assessments, particularly in understudied dry forest systems.[126,127]

However, the limited number of plots in our study constrains statistical power and reduces the robustness of broader generalizations. Accordingly, our reported carbon stock values should be viewed as preliminary baselines or reference points for hypothesis generation rather than definitive landscape-level estimates. Future studies incorporating a greater number of plots per subtype and replication across multiple years would enhance the reliability of extrapolations and allow more rigorous estimation of uncertainty.

Beyond sampling intensity considerations, the physical characteristics of tropical dry forest soils pose additional challenges for accurate measurement. Coarse fragments and abundant root material can introduce bias in soil bulk density (SBD) measurements, particularly when using standard core sampling techniques.[128,129] Furthermore, the shallow, rocky soils typical of these forests present additional challenges for consistent core extraction and accurate volume determination, potentially introducing additional error in SBD estimation.

Timing of sampling constitutes another potential source of bias. Tropical dry forests exhibit strong seasonal moisture fluctuations, so the timing of soil sampling relative to rainfall events can significantly influence soil moisture content and thus the measured bulk density.[130] Even slight differences in sampling dates between sites or seasons could lead to noticeable variations in SBD. Additionally, unquantified disturbances—such as the animal activity observed at the LSF and SPF sites—acted as uncontrolled variables that may systematically bias some site or seasonal comparisons. Because the extent and timing of these disturbances were not quantified, their effects could not be accounted for statistically.

Analytical precision in the laboratory further limits the resolution of our findings. Instrumental uncertainties – including those associated with analytical balances, volumetric measurements, and oven temperature stability – introduce a margin of error into soil metrics.[131,132] While our gravimetric method was sensitive enough to detect subtle variations in SBD,

Open Access Article. Published on 15 August 2025. Downloaded on 2/27/2026 8:14:49 PM.
This article is licensed under a Creative Commons Attribution-NonCommercial 3.0 Unported Licence.

the accumulation of small measurement errors might still mask ecologically meaningful differences between treatments or depths.

Finally, our study's chronosequence approach—comparing forests of different ages and disturbance histories—assumes similar initial conditions and developmental trajectories across sites. In reality, site-specific differences in geological substrate, microclimate and past disturbance regimes may violate this assumption.[133,134] Consequently, some differences attributed to forest age or successional stage might reflect inherent site conditions rather than the effects of time or management alone.

4 Conclusions

Carbon dynamics across the three tropical dry forest subtypes revealed distinct patterns, with soil organic carbon (SOC) constituting the dominant pool, followed by aboveground biomass carbon and litterfall carbon. The Jama-Zapotillo Lowland Semideciduous Forest consistently exhibited superior carbon storage capacity, while the Deciduous Pacific Forest of the Equatorial Coast showed the lowest stocks, demonstrating the critical influence of forest structure on carbon distribution. Seasonal variability emerged as a key driver of carbon dynamics, particularly affecting litterfall production during rainy periods, reflecting the pronounced climatic sensitivity characteristic of tropical dry ecosystems.

SOC represents the most substantial and stable carbon reservoir in these forests, with significant contributions from deeper soil layers that are often overlooked in carbon assessments. The persistent carbon storage at 40–80 cm depth emphasizes the necessity of comprehensive soil sampling protocols to avoid systematic underestimation of ecosystem carbon potential. This finding underscores the fundamental role of soils as primary carbon sinks in tropical dry forest ecosystems.

Climatic periodicity strongly influences all carbon components, with enhanced productivity and carbon cycling during rainy seasons reflecting the dynamic nature of these seasonally-driven ecosystems. These temporal variations are intrinsically linked to biodiversity patterns and ecosystem functionality, highlighting the complex interactions between climate, carbon dynamics, and ecological processes in tropical dry forests.

The strategic importance of comprehensive carbon monitoring in Ecuadorian coastal dry forests extends beyond scientific understanding to inform climate change mitigation and adaptation strategies. These ecosystems function as significant carbon sinks while remaining highly vulnerable to anthropogenic pressures, including agricultural conversion and livestock impacts. Effective conservation requires targeted policies that prioritize preventive management, maximize carbon sequestration potential, and strengthen ecosystem resilience.

This research advances understanding of carbon dynamics in understudied tropical dry forest subtypes, demonstrating their critical role in global carbon storage and biodiversity conservation. Effective management and preservation of these forests are essential for maintaining their carbon sequestration services and ensuring their continued contribution to climate change mitigation efforts.

Author contributions

Michael Macías-Pro: methodology, investigation, formal analysis, original drafting, visualization, writing – review and editing. Emilio Jarre Castro: methodology, investigation, writing – review and editing. Juan Manuel Moreira Castro: methodology, investigation, formal analysis. José Montoya Terán: conceptualization, resources, supervision, writing – review and editing, funding acquisition. Ezequiel Zamora-Ledezma: conceptualization, investigation, formal analysis, resources, supervision, original drafting, writing – review and editing, project administration, funding acquisition.

Conflicts of interest

The authors declare no conflict of interest in this work.

Data availability

Substantial CASA data are available at **https://osf.io/tskc2/?view_only=a1866f9a94144cbd8a0bb34fdcc8dd7b**. Additional data are available upon request, and through forthcoming publications.

Geographic coordinates of plots, boxplots of soil properties, species lists per forest type and climatic period, contributions of species to aboveground carbon, seasonal litterfall data, and detailed SOC, CAGB, and C-litterfall measurements across tropical dry forest subtypes. See DOI: **https://doi.org/10.1039/d5va00018a**.

Acknowledgements

The authors would like to thank the French Embassy in Ecuador, the FSPI – Solidarity Fund for Innovative Projects of the French Ministry for Europe and Foreign Affairs (MEAE), and the Technical University of Manabí for their support and co-financing of the doctoral study program of Michael A. Macias Pro.

Notes and references

1 A. Baccini, W. Walker, L. Carvalho, M. Farina, D. Sulla-Menashe and R. A. Houghton, Tropical forests are a net carbon source based on aboveground measurements of gain and loss, *Science*, 2017, **358**, 230–234.
2 G. Tsegay and X. Z. Meng, Impact of Ex-Closure in above and below Ground Carbon Stock Biomass, *Forests*, 2021, **12**, 130.
3 D. S. Schimel, Terrestrial ecosystems and the carbon cycle, *Global Change Biol.*, 1995, **1**, 77–91.
4 M. Hari and B. Tyagi, Terrestrial carbon cycle: tipping edge of climate change between the atmosphere and biosphere ecosystems, *Environ. Sci.: Atmos.*, 2022, **2**, 867–890.
5 B. Baboo, R. Sagar, S. S. Bargali and H. verma, *Tree Species Composition, Regeneration and Diversity of an Indian Dry Tropical Forest Protected Area*, 2017.

 © 2025 The Author(s). Published by the Royal Society of Chemistry

Open Access Article. Published on 15 August 2025. Downloaded on 2/27/2026 8:14:49 PM.
This article is licensed under a Creative Commons Attribution-NonCommercial 3.0 Unported Licence.

6 E. O. Wilson and F. M. Peter, *The Current State of Biological Diversity*, 1988, https://www.ncbi.nlm.nih.gov/books/NBK219273/, accessed 31 July 2025.
7 B. H. Kittur, S. L. Swamy, S. S. Bargali and M. K. Jhariya, Wildland fires and moist deciduous forests of Chhattisgarh, India: divergent component assessment, *J. For. Res.*, 2014, **25**, 857–866.
8 N. Z. Htun, N. Mizoue and S. Yoshida, Tree species composition and diversity at different levels of disturbance in Popa Mountain Park, Myanmar, *Biotropica*, 2011, **43**, 597–603.
9 W. Hubau, S. L. Lewis, O. L. Phillips, K. Affum-Baffoe, H. Beeckman, A. Cuní-Sanchez, *et al.*, Asynchronous carbon sink saturation in African and Amazonian tropical forests, *Nature*, 2020, **579**, 80–87.
10 T. Sunderland, D. Apgaua, C. Baldauf, R. Blackie, C. Colfer, A. B. Cunningham, *et al.*, Global dry forests: a prologue, *Int. For. Rev.*, 2015, **17**, 1–9.
11 M. Dimson and T. W. Gillespie, Trends in active restoration of tropical dry forest: Methods, metrics, and outcomes, *For. Ecol. Manage.*, 2020, **467**, 118150.
12 C. A. Rivas, J. Guerrero-Casado and R. M. Navarro-Cerillo, Deforestation and fragmentation trends of seasonal dry tropical forest in Ecuador: impact on conservation, *For. Ecosyst.*, 2021, **8**, 46.
13 Z. G. Siyum, Tropical dry forest dynamics in the context of climate change: syntheses of drivers, gaps, and management perspectives, *Ecol. Process*, 2020, **9**, 1–16.
14 L. Miles, A. C. Newton, R. S. DeFries, C. Ravilious, I. May, S. Blyth, *et al.*, A global overview of the conservation status of tropical dry forests, *J. Biogeogr.*, 2006, **33**, 491–505.
15 C. Rankine, A. Sanchez-Azofeifa, M. M. do Espirito-Santo and K. Stan, Succession and seasonality of a Brazilian secondary tropical dry forest: Phenology and climate moderation, *For. Ecol. Manage.*, 2024, **568**, 122151.
16 M. F. Fernandes, D. Cardoso and L. P. de Queiroz, An updated plant checklist of the Brazilian Caatinga seasonally dry forests and woodlands reveals high species richness and endemism, *Alger. J. Arid Environ.*, 2020, **174**, 104079.
17 Y. Ren, F. Lin, C. Jiang, J. Tang, Z. Fan, D. Feng, *et al.*, Understory vegetation management regulates soil carbon and nitrogen storage in rubber plantations, *Nutr. Cycling Agroecosyst.*, 2023, **127**, 209–224.
18 Y. Liu, K. Wang, L. Dong, J. Li, X. Wang, Z. Shangguan, *et al.*, Dynamics of litter decomposition rate and soil organic carbon sequestration following vegetation succession on the Loess Plateau, China, *Catena*, 2023, **229**, 107225.
19 A. Barik and S. Baidya Roy, Climate change strongly affects future fire weather danger in Indian forests, *Commun. Earth Environ.*, 2023, **4**, 1–14.
20 N. Forero-Chavez, A. Arenas-Clavijo, I. Armbrecht and J. Montoya-Lerma, Urban patches of dry forest as refuges for ants and carabid beetles in a neotropical overcrowded city, *Urban Ecosyst*, 2024, **27**, 1263–1278.
21 C. Andrade Díaz, A. Albers, E. Zamora-Ledezma and L. Hamelin, The interplay between bioeconomy and the maintenance of long-term soil organic carbon stock in agricultural soils: A systematic review, *Renewable Sustainable Energy Rev.*, 2024, **189**, 113890.
22 S. S. Dhaliwal, R. K. Naresh, A. Mandal, R. Singh and M. K. Dhaliwal, Dynamics and transformations of micronutrients in agricultural soils as influenced by organic matter build-up: A review, *Environ. Sustain. Indic.*, 2019, **1–2**, 100007.
23 Q. He, D. L. Liu, B. Wang, A. Cowie, A. Simmons, C. Waters, L. Li, P. Feng, Y. Li, P. de Voil, A. Huete and Q. Yu, Modelling interactions between cowpea cover crops and residue retention in Australian dryland cropping systems under climate change, *Agric., Ecosyst. Environ.*, 2023, **353**, 108536.
24 C. Andrade Díaz, H. Clivot, A. Albers, E. Zamora-Ledezma and L. Hamelin, The crop residue conundrum: Maintaining long-term soil organic carbon stocks while reinforcing the bioeconomy, compatible endeavors?, *Appl. Energy*, 2023, **329**, 120192.
25 R. Lal, C. Monger, L. Nave and P. Smith, The role of soil in regulation of climate, *Philos. Trans. R. Soc., B*, 2021, **376**, 20210084.
26 E. Zamora-Ledezma, P. M. Macías, E. Jarre Castro, J. Vera Vélez, R. Briones Saltos, J. Vélez Velásquez, *et al.*, Advancing carbon quantification: a comparative evaluation of gravimetric and volumetric methods for soil carbon assessment in tropical ecosystems, *Results Eng.*, 2025, 104141.
27 K. Stan and A. Sanchez-Azofeifa, Tropical Dry Forest Diversity, Climatic Response, and Resilience in a Changing Climate, *Forests*, 2019, **10**, 443.
28 A. G. S. Menezes, S. R. M. Lins, C. S. G. Silva, M. Tabarelli and B. K. C. Filgueiras, Negative effects of human disturbance and increased aridity on root biomass and nutrients along the regeneration of a tropical dry forest in the context of slash-and-burn agriculture, *Sci. Total Environ.*, 2024, **934**, 172955.
29 H. Li, B. Yang, Y. Meng, K. Liu, S. Wang, D. Wang, H. Zhang, Y. Huang, X. Liu, D. Li, *et al.*, Relationship between carbon pool changes and environmental changes in arid and semi-arid steppe—A two decades study in Inner Mongolia, China, *Sci. Total Environ.*, 2023, **893**, 164930.
30 W. Sun, J. G. Canadell, L. Yu, L. Yu, W. Zhang, P. Smith, *et al.*, Climate drives global soil carbon sequestration and crop yield changes under conservation agriculture, *Global Change Biol.*, 2020, **26**, 3325–3335.
31 X. Zhu, J. Si, B. Jia, X. He, D. Zhou, C. Wang, *et al.*, Changes of soil carbon along precipitation gradients in three typical vegetation types in the Alxa desert region, China, *Carbon Balance Manage.*, 2024, **19**, 1–17.
32 M. Giweta, Role of litter production and its decomposition, and factors affecting the processes in a tropical forest ecosystem: A review, *J. Ecol. Environ. Sci.*, 2020, **44**, 1–9.

Open Access Article. Published on 15 August 2025. Downloaded on 2/27/2026 8:14:49 PM.
This article is licensed under a Creative Commons Attribution-NonCommercial 3.0 Unported Licence.

33 J. Chave, H. C. Muller-Landau and S. A. Levin, Comparing classical community models: Theoretical consequences for patterns of diversity, *Am. Nat.*, 2002, **159**, 1–23.
34 R. Mäkipää, R. Abramoff, B. Adamczyk, V. Baldy, C. Biryol, M. Bosela, *et al.*, How does management affect soil C sequestration and greenhouse gas fluxes in boreal and temperate forests? – a review, *For. Ecol. Manage.*, 2023, **529**, 120637.
35 N. Krüger, D. R. Finn and A. Don, Soil depth gradients of organic carbon-13 – a review on drivers and processes, *Plant Soil*, 2023, **495**(1), 113–136.
36 L. G. Garrett, A. K. Byers, K. Wigley, K. A. Heckman, J. A. Hatten and S. A. Wakelin, Lifting the Profile of Deep Forest Soil Carbon, *Soil Syst.*, 2024, **8**(8), 105.
37 A. D. Agbelade and J. C. Onyekwelu, Tree species diversity, volume yield, biomass and carbon sequestration in urban forests in two Nigerian cities, *Urban Ecosyst*, 2020, **23**, 957–970.
38 H. Morffi-Mestre, G. Ángeles-Pérez, J. S. Powers, J. L. Andrade, A. H. H. Ruiz, F. May-Pat, *et al.*, Multiple Factors Influence Seasonal and Interannual Litterfall Production in a Tropical Dry Forest in Mexico, *Forests*, 2020, **11**, 1241.
39 H. González-Rodríguez, I. C. Silva, R. Gonzalo Ramírez-Lozano, T. Gustavo and D. Gomez, *Spatial and Seasonal Litterfall Deposition Pattern in the Tamaulipan Thorscrub*, Northeastern Mexico, 2008, **https://www.researchgate.net/publication/264041701**, accessed 30 Aug 2023.
40 B. H. J. De Jong, *Spatial Distribution of Biomass and Links to Reported Disturbances in Tropical Lowland Forests of Southern Mexico*, 2014, vol. 4, pp. 601–615.
41 V. Smith, C. Portillo-Quintero, A. Sanchez-Azofeifa and J. L. Hernandez-Stefanoni, Assessing the accuracy of detected breaks in Landsat time series as predictors of small scale deforestation in tropical dry forests of Mexico and Costa Rica, *Remote Sens. Environ.*, 2019, **221**, 707–721.
42 S. Zhao and M. Riaz, Plant–Soil Interactions and Nutrient Cycling Dynamics in Tropical Rainforests, *Environment, Climate, Plant and Vegetation Growth*, 2024, pp. 229–264.
43 K. D. Stan, A. Sanchez-Azofeifa and H. F. Hamann, Widespread degradation and limited protection of forests in global tropical dry ecosystems, *Biol. Conserv.*, 2024, **289**, 110425.
44 L. Cervera, D. J. Lizcano, D. G. Tirira and G. Donati, Surveying Two Endangered Primate Species (Alouatta palliata aequatorialis and Cebus aequatorialis) in the Pacoche Marine and Coastal Wildlife Refuge, West Ecuador, *Int. J. Primatol.*, 2015, **36**, 933–947.
45 *Geografía Y Clima*, **https://bioweb.bio/fungiweb/GeografiaClima/**, accessed 16 Aug 2023.
46 H. A. M. Zhofre, *MAE/FAO. Especies Forestales de los Bosques Secos del Ecuador*, Quito, 2012, **https://enf.ambiente.gob.ec/web_enf/documentos/especiesForestalesBosqueSeco.pdf**, accessed 15 Dec 2024.
47 *ISO 11461:2001 – Soil Quality—Determination of Soil Water Content as a Volume Fraction Using Coring Sleeves—Gravimetric Method*, **https://www.iso.org/standard/33031.html**, accessed 21 Aug 2023.
48 UNE 77308:2001 Calidad del suelo, *Determinación de la conducti*, **https://www.une.org/encuentra-tu-norma/busca-tu-norma/norma?c=N0024111**, accessed 21 Aug 2023.
49 UNE, Lodos, suelos y residuos biológicos tratados, *Determinación del pH (ISO 10390:2021)*, 2022, **https://enf.ambiente.gob.ec/web_enf/documentos/especiesForestalesBosqueSeco.pdf**, accessed 15 Dec 2024.
50 J. Chave, C. Andalo, S. Brown, M. A. Cairns, J. Q. Chambers, D. Eamus, *et al.*, Tree allometry and improved estimation of carbon stocks and balance in tropical forests, *Oecologia*, 2005, **145**, 87–99.
51 J. Chave, D. Coomes, S. Jansen, S. L. Lewis, N. G. Swenson and A. E. Zanne, Towards a worldwide wood economics spectrum, *Soil Ecol. Lett.*, 2009, **12**, 351–366.
52 J. Penman, M. Gytarsky, T. Hiraishi, T. Krug, D. Kruger, R. Pipatti, *et al.*, Intergovernmental Panel on Climate Change Good Practice Guidance for Land Use, *Land-Use Change and Forestry IPCC National Greenhouse Gas Inventories Programme*, Published by the Institute for Global Environmental Strategies (IGES) for the IPCC, 2023, **http://www.ipcc-nggip.iges.or.jp**.
53 E. N. Honorio Coronado and T. R. Baker, *Manual para el monitoreo del ciclo del carbono en bosques amazónicos*, Instituto de Investigaciones de la Amazonía Peruana/Universidad de Leeds, Lima, 2010, p. 54.
54 A. Walkley and I. A. Black, An examination of the degtjareff method for determining soil organic matter, and a proposed modification of the chromic acid titration method, *Soil Sci.*, 1934, **37**, 29–38.
55 T. B. Bruun, K. Egay, O. Mertz and J. Magid, Improved sampling methods document decline in soil organic carbon stocks and concentrations of permanganate oxidizable carbon after transition from swidden to oil palm cultivation, *Agric., Ecosyst. Environ.*, 2013, **178**, 127–134.
56 Posit team, *RStudio: Integrated Development Environment for R*, 2024.
57 Ø. Hammer, D. A. T. Harper and P. D. Ryan, *PAST: Paleontological Statistics Software Package*, 2024.
58 M. Busse, J. Zhang, G. Fiddler and D. Young, Compaction and organic matter retention in mixed-conifer forests of California: 20-year effects on soil physical and chemical health, *For. Ecol. Manage.*, 2021, **482**, 118851.
59 P. Dłużewski, K. Wiatrowska and S. Kuśmierz, The Role of Stand Age in Soil Carbon Dynamics in Afforested Post-Agricultural Ecosystems: The Case of Scots Pine Forests in Dfb-Climate Zone, *Forests*, 2024, **15**, 2127.
60 R. Pandey, S. S. Bargali, K. Bargali, H. Karki and R. K. Chaturvedi, Dynamics of nitrogen mineralization and fine root decomposition in sub-tropical Shorea robusta Gaertner f. forests of Central Himalaya, India, *Sci. Total Environ.*, 2024, **921**, 170896.
61 A. Fartyal, S. S. Bargali, K. Bargali and B. Negi, Changes in Soil Properties, Organic Carbon, and Nutrient Stocks After

 © 2025 The Author(s). Published by the Royal Society of Chemistry

Open Access Article. Published on 15 August 2025. Downloaded on 2/27/2026 8:14:49 PM.
This article is licensed under a Creative Commons Attribution-NonCommercial 3.0 Unported Licence.

Land-Use Change From Forests to Grasslands in Kumaun Himalaya, India, *Land Degrad. Dev.*, 2025, **36**, 2438–2457.
62 V. Bisht, S. Sharma, S. S. Bargali and A. Fartyal, Topographic and Edaphic Factors Shaping Floral Diversity Patterns and Vegetation Structure of Treeline Ecotones in Kumaun Himalaya, *Land Degrad. Dev.*, 2025, **36**, 4260–4280.
63 K. Bargali, V. Manral, K. Padalia, S. S. Bargali and V. P. Upadhyay, Effect of vegetation type and season on microbial biomass carbon in Central Himalayan forest soils, India, *Catena*, 2018, **171**, 125–135.
64 U. Schickhoff, *Nepal: an Introduction to the Natural History, Ecology and Human Environment of the Himalayas. A Companion to the Flora of Nepal*, ed. G. Miehe, C. Pendry and R. Chaudhary, Edinb J. Bot, 2017, vol. 74, pp. 370–373.
65 X. Gao, S. M. Rodrigues, E. Spielman-Sun, S. Lopes, S. Rodrigues, Y. Zhang, *et al.*, Effect of Soil Organic Matter, Soil pH, and Moisture Content on Solubility and Dissolution Rate of CuO NPs in Soil, *Environ. Sci. Technol.*, 2019, **53**, 4959–4967.
66 D. J. Levy-Booth, I. J. W. Giesbrecht, C. T. E. Kellogg, T. J. Heger, D. V. D'Amore, P. J. Keeling, *et al.*, Seasonal and ecohydrological regulation of active microbial populations involved in DOC, CO2, and CH4 fluxes in temperate rainforest soil, *ISME J.*, 2019, **13**, 950–963.
67 M. C. A. Salas, J. C. Alegre Orihuela and A. S. Iglesias, Estimation of above-ground live biomass and carbon stocks in different plant formations and in the soil of dry forests of the Ecuadorian coast, *Food Energy Secur.*, 2017, **6**, e00115.
68 N. T. Lepcha and N. B. Devi, Effect of land use, season, and soil depth on soil microbial biomass carbon of Eastern Himalayas, *Ecol. Process*, 2020, **9**, 1–14.
69 Z. Zhao, G. Liu, Q. Liu, C. Huang, H. Li and C. Wu, Distribution Characteristics and Seasonal Variation of Soil Nutrients in the Mun River Basin, Thailand, *Int. J. Environ. Res. Public Health*, 2018, **15**, 1818.
70 Z. Liu, C. Gao, Z. Yan, L. Shao, S. Chen, J. Niu, *et al.*, Effects of long-term saline water irrigation on soil salinity and crop production of winter wheat-maize cropping system in the North China Plain: A case study, *Agric. Water Manag.*, 2024, **303**, 109060.
71 A. A. Agbeshie, S. Abugre, T. Atta-Darkwa and R. Awuah, A review of the effects of forest fire on soil properties, *J. For. Res.*, 2022, **33**, 1419–1441.
72 Y. Dong, R. Chen, E. Petropoulos, B. Yu, J. Zhang, X. Lin, *et al.*, Interactive effects of salinity and SOM on the ecoenzymatic activities across coastal soils subjected to a saline gradient, *Geoderma*, 2022, **406**, 115519.
73 S. S. Yamaç, C. Şeker and H. Negiş, Evaluation of machine learning methods to predict soil moisture constants with different combinations of soil input data for calcareous soils in a semi arid area, *Agric. Water Manag.*, 2020, **234**, 106121.
74 S. Kurniawan, S. R. Utami, M. Mukharomah, I. A. Navarette and B. Prasetya, Land Use Systems, Soil Texture, Control Carbon and Nitrogen Storages in the Forest Soil of UB Forest, Indonesia, *Agrivita J. Agricultural Sci.*, 2019, **41**, 416–427.
75 J. Huang and A. E. Hartemink, Soil and environmental issues in sandy soils, *Earth-Sci. Rev.*, 2020, **208**, 103295.
76 C. W. W. Ng and D. Peprah-Manu, Pore structure effects on the water retention behaviour of a compacted silty sand soil subjected to drying-wetting cycles, *Eng. Geol.*, 2023, **313**, 106963.
77 M. S. Ross, C. L. Coultas and Y. P. Hsieh, Soil-productivity relationships and organic matter turnover in dry tropical forests of the Florida Keys, *Plant Soil*, 2003, **253**, 479–492.
78 L. L. de Sosa, I. Carmona, M. Panettieri, D. M. Griffith, C. I. Espinosa, A. Jara-Guerrero, *et al.*, Ecosystem function associated with soil organic carbon declines with tropical dry forest degradation, *Land Degrad. Dev.*, 2024, **35**, 2109–2121.
79 F. Marinho, F. Oehl, I. R. da Silva, D. Coyne, J. S. da N. Veras and L. C. Maia, High diversity of arbuscular mycorrhizal fungi in natural and anthropized sites of a Brazilian tropical dry forest (Caatinga), *Fungal Ecol.*, 2019, **40**, 82–91.
80 M. K. Jhariya and L. Singh, Effect of fire severity on soil properties in a seasonally dry forest ecosystem of Central India, *Int. J. Environ. Sci. Technol.*, 2021, **18**, 3967–3978.
81 M. K. Jhariya and L. Singh, Effect of fire severity on soil properties in a seasonally dry forest ecosystem of Central India, *Int. J. Environ. Sci. Technol.*, 2021, **18**, 3967–3978.
82 P. C. Salazar, R. M. Navarro-Cerrillo, N. Grados, G. Cruz, V. Barrón and R. Villar, Leaf nutrients in Prosopis pallida are determined by soil chemical attributes under eutric conditions in a dryland forest, *Trees-Struct. Funct.*, 2021, **35**, 375–386.
83 C. Chen, H. Y. H. Chen, X. Chen and Z. Huang, Meta-analysis shows positive effects of plant diversity on microbial biomass and respiration, *Nat. Commun.*, 2019, **10**, 1–10.
84 J. Liang, T. W. Crowther, N. Picard, S. Wiser, M. Zhou, G. Alberti, *et al.*, Positive biodiversity-productivity relationship predominant in global forests, *Science*, 2016, **354**(6309), 196.
85 A. I. García-Cervigón, J. J. Camarero, E. Cueva, C. I. Espinosa and A. Escudero, Climate seasonality and tree growth strategies in a tropical dry forest, *J. Veg. Sci.*, 2020, **31**, 266–280.
86 C. M. Smith-Martin, X. Xu, D. Medvigy, S. A. Schnitzer and J. S. Powers, Allometric scaling laws linking biomass and rooting depth vary across ontogeny and functional groups in tropical dry forest lianas and trees, *New Phytol.*, 2020, **226**, 714–726.
87 K. M. Bordin, A. Esquivel-Muelbert, R. S. Bergamin, J. Klipel, R. C. Picolotto, M. A. Frangipani, *et al.*, Climate and large-sized trees, but not diversity, drive above-ground biomass in subtropical forests, *For. Ecol. Manage.*, 2021, **490**, 119126.
88 Z. Yuan, A. Ali, A. Sanaei, P. Ruiz-Benito, T. Jucker, L. Fang, *et al.*, Few large trees, rather than plant diversity and composition, drive the above-ground biomass stock and

Open Access Article. Published on 15 August 2025. Downloaded on 2/27/2026 8:14:49 PM.
This article is licensed under a Creative Commons Attribution-NonCommercial 3.0 Unported Licence.

dynamics of temperate forests in northeast China, *For. Ecol. Manage.*, 2021, **481**, 118698.

89 C. Piponiot, K. J. Anderson-Teixeira, S. J. Davies, D. Allen, N. A. Bourg, D. F. R. P. Burslem, *et al.*, Distribution of biomass dynamics in relation to tree size in forests across the world, *New Phytol.*, 2022, **234**, 1664–1677.

90 H. K. Viana Santos, R. Borges de Lima, R. L. Figueiredo de Souza, D. Cardoso, P. W. Moonlight, T. Teixeira Silva, C. Pereira de Oliveira, F. T. Alves Júnior, E. Veenendaal, L. P. de Queiroz, P. M. S. Rodrigues, R. M. dos Santos, T. Sarkinen, A. de Paula, P. A. B. Barreto-Garcia, T. Pennington and O. L. Phillips, Spatial distribution of aboveground biomass stock in tropical dry forest in Brazil, *iFor. Biogeosci. For.*, 2023, **16**, 116–126.

91 T. Dalgleish, J. M. G. Williams, A.-M. J. Golden, N. Perkins, L. F. Barrett, P. J. Barnard, *et al.*, Protocolo para la estimación nacional y subnacional de biomasa – carbono en Colombia, *J. Exp. Psychol.*, 2007, **136**, 23–42.

92 J. L. Hernández-Stefanoni, M. Á. Castillo-Santiago, J. F. Mas, C. E. Wheeler, J. Andres-Mauricio, F. Tun-Dzul, *et al.*, Improving aboveground biomass maps of tropical dry forests by integrating LiDAR, ALOS PALSAR, climate and field data, *Carbon Balance Manage.*, 2020, **15**, 1–17.

93 C. P. de Oliveira, R. L. C. Ferreira, J. A. A. da Silva, R. B. de Lima, E. A. Silva, A. F. da Silva, *et al.*, Modeling and spatialization of biomass and carbon stock using lidar metrics in tropical dry forest, brazil, *Forests*, 2021, **12**, NA.

94 E. E. Mwakalukwa, H. Meilby and T. Treue, Carbon storage in a dry Miombo woodland area in Tanzania, *J. For. Sci.*, 2024, **86**, 115–124.

95 D. G. Souza, J. C. Sfair, A. S. de Paula, M. F. Barros, K. F. Rito and M. Tabarelli, Multiple drivers of aboveground biomass in a human-modified landscape of the Caatinga dry forest, *For. Ecol. Manage.*, 2019, **435**, 57–65.

96 R. C. d. Santos, R. V. O. Castro, A. D. C. O. Carneiro, A. F. N. M. Castro, A. S. Pimenta, E. M. Pinto, *et al.*, Estoques de volume, biomassa e carbono na madeira de espécies da Caatinga em Caicó, RN, *Pesquisa Florestal Brasileira*, 2016, **36**, 1.

97 P. Daleo, J. Alberti, E. J. Chaneton, O. Iribarne, P. M. Tognetti, J. D. Bakker, *et al.*, Environmental heterogeneity modulates the effect of plant diversity on the spatial variability of grassland biomass, *Nat. Commun.*, 2023, **14**, 1–11.

98 J. Dolezal, P. Fibich, J. Altman, J. Leps, S. Uemura, K. Takahashi, *et al.*, Determinants of ecosystem stability in a diverse temperate forest, *Oikos*, 2020, **129**, 1692–1703.

99 H. Morffi-Mestre, G. Ángeles-Pérez, J. S. Powers, J. L. Andrade, A. H. H. Ruiz, F. May-Pat, *et al.*, Multiple Factors Influence Seasonal and Interannual Litterfall Production in a Tropical Dry Forest in Mexico, *Forests*, 2020, **11**, 1241.

100 D. R. Aryal, B. H. J. De Jong, S. Ochoa-Gaona, J. Mendoza-Vega and L. Esparza-Olguin, Successional and seasonal variation in litterfall and associated nutrient transfer in semi-evergreen tropical forests of SE Mexico, *Nutr. Cycling Agroecosyst.*, 2015, **103**, 45–60.

101 A. Ali, S. L. Lin, J. K. He, F. M. Kong, J. H. Yu and H. S. Jiang, Big-sized trees overrule remaining trees' attributes and species richness as determinants of aboveground biomass in tropical forests, *Global Change Biol.*, 2019, **25**, 2810–2824.

102 D. L. Machado, V. L. Engel, D. S. Podadera, L. M. Sato, R. G. M. de Goede, L. F. D. de Moraes, *et al.*, Site and plant community parameters drive the effect of vegetation on litterfall and nutrient inputs in restored tropical forests, *Plant Soil*, 2021, **464**, 405–421.

103 A. Martínez-Yrízar and J. Sarukhán, Litterfall Patterns in a Tropical Deciduous Forest in Mexico Over a Five-Year Period, *J. Trop. Ecol.*, 1990, **6**, 433–444.

104 D. Marod, T. Nakashizuka, T. Saitoh, K. Hirai, S. Thinkampheang, L. Asanok, *et al.*, Long Term Seasonal Variability on Litterfall in Tropical Dry Forests, Western Thailand, *Forests*, 2023, **14**, 2107.

105 J. S. Powers and E. Veldkamp, Regional variation in soil carbon and δ13C in forests and pastures of northeastern Costa Rica, *Biogeochemistry*, 2005, **72**, 315–336.

106 J. Castellanos-Barliza, V. Carmona-Escobar, J. Linero-Cueto, E. Ropain-Hernández and J. D. León-Peláez, Fine Litter Dynamics in Tropical Dry Forests Located in Two Contrasting Landscapes of the Colombian Caribbean, *Forests*, 2022, **13**, 660.

107 G. Kassa, T. Bekele, S. Demissew and T. Abebe, Leaves litterfall and nutrient inputs from four multipurpose tree/shrub species of homegarden agroforestry systems, *Environ. Syst. Res.*, 2022, **11**, 1–16.

108 D. Marod, T. Andriyas, N. Leksungnoen, R. Kjelgren, T. | Sathid, P. Chansri, *et al.*, Potential variables forcing litterfall in a lower montane evergreen forest using Granger and superposed epoch analyses, *Ecosphere*, 2023, **14**, e4572.

109 V. C. Smith and A. R. Ennos, The effects of air flow and stem flexure on the mechanical and hydraulic properties of the stems of sunflowers Helianthus annuus L, *J. Exp. Bot.*, 2003, **54**, 845–849.

110 Q. Wu, F. Wu, J. Zhu and X. Ni, Leaf and root inputs additively contribute to soil organic carbon formation in various forest types, *J. Soils Sediments*, 2023, **23**, 1135–1145.

111 P. J. Gregory, RUSSELL REVIEW Are plant roots only "in" soil or are they "of" it? Roots, soil formation and function, *Eur. J. Soil Sci.*, 2022, **73**, e13219.

112 J. Dong, K. Zhou, P. Jiang, J. Wu and W. Fu, Revealing horizontal and vertical variation of soil organic carbon, soil total nitrogen and C:N ratio in subtropical forests of southeastern China, *J. Environ. Manage.*, 2021, **289**, 112483.

113 A. Gholizadeh, R. A. Viscarra Rossel, M. Saberioon, L. Borůvka, J. Kratina and L. Pavlů, National-scale spectroscopic assessment of soil organic carbon in forests of the Czech Republic, *Geoderma*, 2021, **385**, 114832.

114 L. L. d. S. Almeida, L. A. Frazão, T. A. M. Lessa, L. A. Fernandes, L. d. C. Veloso, A. M. Q. Lana, *et al.*, Soil carbon and nitrogen stocks and the quality of soil organic matter under silvopastoral systems in the Brazilian Cerrado, *Soil Tillage Res.*, 2021, **205**, 104785.

 © 2025 The Author(s). Published by the Royal Society of Chemistry

Open Access Article. Published on 15 August 2025. Downloaded on 2/27/2026 8:14:49 PM.
This article is licensed under a Creative Commons Attribution-NonCommercial 3.0 Unported Licence.

115 C. d. R. Ferreira, E. C. d. Silva Neto, M. G. Pereira, J. d. N. Guedes, J. S. Rosset and L. H. C. d. Anjos, Dynamics of soil aggregation and organic carbon fractions over 23 years of no-till management, *Soil Tillage Res.*, 2020, **198**, 104533.

116 S. L. Bellè, J. Riotte, M. Sekhar, L. Ruiz, M. Schiedung and S. Abiven, Soil organic carbon stocks and quality in small-scale tropical, sub-humid and semi-arid watersheds under shrubland and dry deciduous forest in southwestern India, *Geoderma*, 2022, **409**, 115606.

117 S. Singh, M. A. Mayes, A. Shekoofa, S. N. Kivlin, S. Bansal and S. Jagadamma, Soil organic carbon cycling in response to simulated soil moisture variation under field conditions, *Sci. Rep.*, 2021, **11**, 1–13.

118 S. Kumar and L. K. Sharma, Assessing spatial and seasonal variability in soil organic carbon fractions of teal carbon in semi-arid Ramsar wetlands of India as a natural climate solution, *Discov. Soil*, 2025, **2**, 1–17.

119 S. W. Stoner, M. Schrumpf, A. Hoyt, C. A. Sierra, S. Doetterl, V. Galy, *et al.*, How well does ramped thermal oxidation quantify the age distribution of soil carbon? Assessing thermal stability of physically and chemically fractionated soil organic matter, *Biogeosciences*, 2023, **20**, 3151–3163.

120 M. Satdichanh, G. G. O Dossa, K. Yan, K. W. Tomlinson, K. E. Barton, S. E. Crow, *et al.*, Drivers of soil organic carbon stock during tropical forest succession, *J. Ecol.*, 2023, 1–13.

121 D. Raha, J. A. Dar, P. K. Pandey, P. A. Lone, S. Verma, P. K. Khare, *et al.*, Variation in tree biomass and carbon stocks in three tropical dry deciduous forest types of Madhya Pradesh, India, *Carbon Manage.*, 2020, **11**, 109–120.

122 J. G. López-Santiago, F. Casanova-Lugo, G. Villanueva-López, V. F. Díaz-Echeverría, F. J. Solorio-Sánchez, P. Martínez-Zurimendi, *et al.*, Carbon storage in a silvopastoral system compared to that in a deciduous dry forest in Michoacán, Mexico, *Agrofor. Syst.*, 2019, **93**, 199–211.

123 V. A. Maia, A. B. Miranda Santos, N. de Aguiar-Campos, C. R. de Souza, M. C. F. de Oliveira, P. A. Coelho, *et al.*, The carbon sink of tropical seasonal forests in southeastern Brazil can be under threat, *Sci. Adv.*, 2020, **6**(51), eabd4548.

124 K. Srinivas and S. Sundarapandian, Biomass and carbon stocks of trees in tropical dry forest of East Godavari region, Andhra Pradesh, India, *Geol. Ecol. Landsc.*, 2019, **3**, 114–122.

125 J. Pelletier, A. Paquette, K. Mbindo, N. Zimba, A. Siampale, B. Chendauka, *et al.*, Carbon sink despite large deforestation in African tropical dry forests (miombo woodlands), *Environ. Res. Lett.*, 2018, **13**, 094017.

126 A. Rivero-Villar, M. de la Peña-Domene, G. Rodríguez-Tapia, C. P. Giardina and J. Campo, A Pantropical Overview of Soils across Tropical Dry Forest Ecoregions, *Sustainability*, 2022, **14**, 6803.

127 J. Grace, E. Mitchard and E. Gloor, Perturbations in the carbon budget of the tropics, *Global Change Biol.*, 2014, **20**, 3238.

128 Q. Chen, S. Cheng, S. Yu, X. Guo, Z. Sun, Z. Hu, *et al.*, Forest restoration in tropical forests recovers topsoil water retention but does not improve deep soil layers, *Int. Soil Water Conserv. Res.*, 2025, DOI: **10.1016/J.ISWCR.2025.05.002**.

129 L. Rodriguez, M. Bastidas, M. Da Silva, J. Arias, J. M. Martín-López, N. Matiz-Rubio, *et al.*, Comparative assessment of soil bulk density measurements using core metal ring and power probe methods in acidic soils of Colombian pasturelands, *Front. Soil Sci.*, 2025, **5**, 1527807.

130 M. L. Vargas-Terminel, D. Flores-Rentería, Z. M. Sánchez-Mejía, N. E. Rojas-Robles, M. Sandoval-Aguilar, B. Chávez-Vergara, *et al.*, Soil Respiration Is Influenced by Seasonality, Forest Succession and Contrasting Biophysical Controls in a Tropical Dry Forest in Northwestern Mexico, *Soil Syst.*, 2022, **6**, 75.

131 J. D. Jabro, W. B. Stevens, W. M. Iversen, J. D. Jabro, W. B. Stevens and W. M. Iversen, Comparing Two Methods for Measuring Soil Bulk Density and Moisture Content, *Open J. Soil Sci.*, 2020, **10**, 233–243.

132 N. H. Batjes, *Procedures and Standards in Use at ISRIC WDC-Soils*, 2022, DOI: **10.17027/isric-wdcsoils-202201**.

133 R. L. Chazdon, S. G. Letcher, M. Van Breugel, M. Martínez-Ramos, F. Bongers and B. Finegan, Rates of change in tree communities of secondary Neotropical forests following major disturbances, *Philos. Trans. R. Soc., B*, 2006, **362**, 273.

134 L. Poorter, D. Craven, C. C. Jakovac, M. T. van der Sande, L. Amissah, F. Bongers, *et al.*, Multidimensional tropical forest recovery, *Science*, 2021, **374**, 1370–1376.